

## ORIGINAL ARTICLE

## EFhd2/Swiprosin-1 is a common genetic determinant for sensation-seeking/low anxiety and alcohol addiction

D Mielenz<sup>1,30</sup>, M Reichel<sup>2,30</sup>, T Jia<sup>3,30</sup>, EB Quinlan<sup>3,30</sup>, T Stöckl<sup>2</sup>, M Mettang<sup>2</sup>, D Zilske<sup>2</sup>, E Kirmizi-Alsan<sup>2</sup>, P Schönberger<sup>2</sup>, M Praetner<sup>2</sup>, SE Huber<sup>2</sup>, D Amato<sup>2</sup>, M Schwarz<sup>4</sup>, P Purohit<sup>1</sup>, S Brachs<sup>5,6</sup>, J Spranger<sup>5,6</sup>, A Hess<sup>7</sup>, C Büttner<sup>8</sup>, AB Ekici<sup>8</sup>, F Perez-Branguli<sup>9</sup>, B Winner<sup>8,9</sup>, V Rauschenberger<sup>10</sup>, T Banaschewski<sup>11</sup>, ALW Bokde<sup>12</sup>, C Büchel<sup>13</sup>, PJ Conrod<sup>14,15</sup>, S Desrivières<sup>16</sup>, H Flor<sup>17</sup>, V Frouin<sup>18</sup>, J Gallinat<sup>19</sup>, H Garavan<sup>20</sup>, P Gowland<sup>21</sup>, A Heinz<sup>22</sup>, J-L Martinot<sup>23</sup>, H Lemaitre<sup>24</sup>, F Nees<sup>17</sup>, T Paus<sup>25</sup>, MN Smolka<sup>26</sup>, IMAGEN Consortium, A Schabony<sup>10</sup>, T Bäuerle<sup>4</sup>, V Eulenburg<sup>27</sup>, C Alzheimer<sup>28</sup>, A Lourdasamy<sup>29</sup>, G Schumann<sup>16,30</sup> and CP Müller<sup>2,30</sup>

In many societies, the majority of adults regularly consume alcohol. However, only a small proportion develops alcohol addiction. Individuals at risk often show a high sensation-seeking/low-anxiety behavioural phenotype. Here we asked which role EF hand domain containing 2 (EFhd2; Swiprosin-1) plays in the control of alcohol addiction-associated behaviours. EFhd2 knockout (KO) mice drink more alcohol than controls and spontaneously escalate their consumption. This coincided with a sensation-seeking and low-anxiety phenotype. A reversal of the behavioural phenotype with  $\beta$ -carboline, an anxiogenic inverse benzodiazepine receptor agonist, normalized alcohol preference in EFhd2 KO mice, demonstrating an EFhd2-driven relationship between personality traits and alcohol preference. These findings were confirmed in a human sample where we observed a positive association of the EFhd2 single-nucleotide polymorphism rs112146896 with lifetime drinking and a negative association with anxiety in healthy adolescents. The lack of EFhd2 reduced extracellular dopamine levels in the brain, but enhanced responses to alcohol. In confirmation, gene expression analysis revealed reduced tyrosine hydroxylase expression and the regulation of genes involved in cortex development, *Eomes* and *Pax6*, in EFhd2 KO cortices. These findings were corroborated in *Xenopus* tadpoles by EFhd2 knockdown. Magnetic resonance imaging (MRI) in mice showed that a lack of EFhd2 reduces cortical volume in adults. Moreover, human MRI confirmed the negative association between lifetime alcohol drinking and superior frontal gyrus volume. We propose that EFhd2 is a conserved resilience factor against alcohol consumption and its escalation, working through *Pax6*/*Eomes*. Reduced EFhd2 function induces high-risk personality traits of sensation-seeking/low anxiety associated with enhanced alcohol consumption, which may be related to cortex function.

*Molecular Psychiatry* (2018) **23**, 1303–1319; doi:10.1038/mp.2017.63; published online 11 April 2017

<sup>1</sup>Division of Molecular Immunology, Department of Internal Medicine III, Nikolaus-Fiebiger-Center, University Clinic, Friedrich-Alexander-University of Erlangen-Nuremberg, Erlangen, Germany; <sup>2</sup>Department of Psychiatry and Psychotherapy, University Clinic, Friedrich-Alexander-University of Erlangen-Nuremberg, Erlangen, Germany; <sup>3</sup>MRC Social, Genetic and Developmental Psychiatry Research Centre, Institute of Psychiatry, King's College London, London, UK; <sup>4</sup>Institute of Radiology, University Medical Center Erlangen, Erlangen, Germany; <sup>5</sup>Department of Endocrinology, Diabetes and Nutrition, Center for Cardiovascular Research, Charité – University School of Medicine, Berlin, Germany; <sup>6</sup>German Center for Cardiovascular Research, DZHK Partner site Berlin, Berlin, Germany; <sup>7</sup>Institute of Experimental and Clinical Pharmacology and Toxicology, Friedrich-Alexander-University Erlangen-Nürnberg, Erlangen, Germany; <sup>8</sup>Institute of Human Genetics, Friedrich-Alexander-Universität Erlangen-Nürnberg, Erlangen, Germany; <sup>9</sup>IZKF Nachwuchsgruppe III, Friedrich-Alexander-University of Erlangen-Nuremberg, Erlangen, Germany; <sup>10</sup>Department of Biology, Developmental Biology, Friedrich-Alexander-University Erlangen-Nuremberg, Erlangen, Germany; <sup>11</sup>Department of Child and Adolescent Psychiatry and Psychotherapy, Central Institute of Mental Health, Medical Faculty Mannheim, Heidelberg University, Mannheim, Germany; <sup>12</sup>Discipline of Psychiatry, School of Medicine and Trinity College Institute of Neuroscience, Trinity College Dublin, Dublin, Ireland; <sup>13</sup>Department of Systems Neuroscience, University Medical Center Hamburg-Eppendorf, Hamburg, Germany; <sup>14</sup>Department of Psychiatry, Université de Montréal, CHU Sainte-Justine Hospital, Montreal, QC, Canada; <sup>15</sup>Department of Psychological Medicine and Psychiatry, Institute of Psychiatry, Psychology & Neuroscience, King's College London, London, UK; <sup>16</sup>Medical Research Council – Social, Genetic and Developmental Psychiatry Centre, Institute of Psychiatry, Psychology & Neuroscience, King's College London, London, UK; <sup>17</sup>Department of Cognitive and Clinical Neuroscience, Central Institute of Mental Health, Medical Faculty Mannheim, Heidelberg University, Mannheim, Germany; <sup>18</sup>Neurospin, Commissariat à l'Energie Atomique, CEA-Saclay Center, Paris, France; <sup>19</sup>Department of Psychiatry and Psychotherapy, University Medical Center Hamburg-Eppendorf (UKE), Hamburg, Germany; <sup>20</sup>Departments of Psychiatry and Psychology, University of Vermont, Burlington, VT, USA; <sup>21</sup>Sir Peter Mansfield Imaging Centre School of Physics and Astronomy, University of Nottingham, University Park, Nottingham, UK; <sup>22</sup>Department of Psychiatry and Psychotherapy, Campus Charité Mitte, Charité, Universitätsmedizin Berlin, Berlin, Germany; <sup>23</sup>Institut National de la Santé et de la Recherche Médicale, INSERM Unit 1000 "Neuroimaging & Psychiatry", University Paris Sud, University Paris Descartes – Sorbonne Paris Cité and Maison de Solenn, Paris, France; <sup>24</sup>Institut National de la Santé et de la Recherche Médicale, INSERM Unit 1000 "Neuroimaging & Psychiatry", Faculté de Médecine, Université Paris-Sud, Le Kremlin-Bicêtre and Université Paris Descartes, Sorbonne Paris Cité, Paris, France; <sup>25</sup>Rotman Research Institute, Baycrest and Departments of Psychology and Psychiatry, University of Toronto, Toronto, ON, Canada; <sup>26</sup>Department of Psychiatry and Neuroimaging Center, Technische Universität Dresden, Dresden, Germany; <sup>27</sup>Institute of Biochemistry, Friedrich-Alexander-University of Erlangen-Nuremberg, Erlangen, Germany; <sup>28</sup>Institute of Physiology and Pathophysiology, Friedrich-Alexander-Universität, Erlangen-Nürnberg, Erlangen, Germany and <sup>29</sup>Division of Child Health, Obstetrics and Gynaecology, School of Medicine, University of Nottingham, Nottingham, UK. Correspondence: Dr CP Müller, Section of Addiction Medicine, Department of Psychiatry and Psychotherapy, University Clinic, Friedrich-Alexander-University Erlangen-Nuremberg, Schwabachanlage 6, Erlangen 91054, Germany. E-mail: Christian.Mueller@uk-erlangen.de

<sup>30</sup>These authors contributed equally to this work

Received 7 October 2016; revised 3 February 2017; accepted 10 February 2017; published online 11 April 2017

## INTRODUCTION

Alcohol addiction is a very common psychiatric disorder with severe health consequences for the individual and detrimental effects for social environment and society.<sup>1</sup> The molecular mechanisms that lead to addiction and those that prevent chronic consumers from such a transition<sup>2,3</sup> are not sufficiently understood.<sup>4</sup> Although symptoms of alcoholism are very similar among affected individuals and well classified in current diagnostic manuals, there are different pathways, which lead from a controlled consumption, which is an accepted part of western society culture,<sup>2,5</sup> to alcohol addiction. Interestingly, only a minority of chronic alcohol consumers of 7–15% develop an addiction.<sup>6–8</sup> Others control their consumption and instrumentalization of the drug over lifetime.<sup>9,10</sup> Thus, there appear risk and resilience factors that make individuals prone or protect them from becoming addicted after they established regular drug consumption. These factors and their neuronal mediators are increasingly considered as predictors and targets for prevention strategies and possibly also for addiction treatment.<sup>11,12</sup>

Gene expression profiles of inbred short sleep vs inbred long sleep mice point towards a potential role of EF hand domain containing 2 (EFhd2, also known as Swiprosin-1) protein coding gene D4Wsu27e as potential resilience factor for alcohol effects on sedation. EFhd2 expression was higher in the cerebellum of inbred long sleep compared to inbred short sleep mice, which were also more sensitive to the sedating effects of alcohol.<sup>13</sup> As a low sensitivity for alcohol effects is associated with higher consumption and increased risk for escalation of consumption, this would suggest that EFhd2 acts as a potential resilience factor against alcohol drinking establishment and possibly addiction.

EFhd2 is a  $\text{Ca}^{2+}$  sensor protein that was originally described in lymphocytes.<sup>14–17</sup> It consists of an N-terminal region of low complexity with an alanine stretch, a functional SH3-binding motif, two functional EF hands and a C-terminal coiled-coil domain.<sup>16,17</sup> EFhd2 binds directly to F-actin and modulates its turnover by control of small GTPases and cofilin, suggesting that it might control synaptic plasticity.<sup>18–21</sup> EFhd2 is abundantly expressed in the human brain.<sup>22</sup> In mice, it is more abundant in adult than in embryonic brain.<sup>23</sup> It is predominantly found in neurons, with highest expression in the cortex and hippocampus, where it is localized in axons, dendrites and synaptic complexes.<sup>22,23</sup> Neurons of EFhd2 knockout (KO) mice show an increased axonal transport and recombinant EFhd2 can inhibit kinesin-mediated microtubule gliding.<sup>23</sup> Knockdown of EFhd2 increases pre-synaptic densities.<sup>22</sup> EFhd2 appears to be associated with various neurodegenerative diseases in mice and humans, which appears to be related to its low expression level in the cortex of dementia patients.<sup>21,22,24,25</sup> In contrast, enhanced cortical EFhd2 protein expression was linked to schizophrenia.<sup>26</sup>

Although the molecular network role of EFhd2 suggests an involvement in behavioural plasticity, little is known about how EFhd2 impacts behaviour and how this translates to a role in psychiatric disorders. We hypothesized that EFhd2 is a resilience factor against the establishment of alcohol addiction-related behaviours, which may work by producing an addiction-prone personality trait by modulating transmitter systems involved in sensation-seeking and anxiety regulation in the brain.<sup>27–29</sup>

## MATERIALS AND METHODS

### Animals

Male and female EFhd2 KO mice on a C57BL/6 background and wild-type (WT) mice<sup>30</sup> were studied in gender-balanced designs. Animals were housed in groups in standard macrolone cages (Type III, Macrolone, Tecniplast, Hohenpeissenberg, Germany), or individually housed in these cages in all drinking studies. They were provided with food and water *ad libitum*, with paper towels as cage enrichment, and kept on a 12:12 h light:dark cycle (lights on at 0700 hours). All mice were tested at an age of

2–6 month, with balanced age/gender in all experiments. Behavioural tests were performed during the light cycle between 0900 and 1600 hours. Room temperature was maintained between 19 and 22 °C at a humidity of 55% ( $\pm 10\%$ ). All behavioural and neurochemical tests were performed by experimenters blind to hypothesis and/or genotype. All experiments were carried out in accordance with the National Institutes of Health guidelines for the humane treatment of animals and the European Communities Council Directive (86/609/EEC) and approved by the local governmental commission for animal health (German state administration Bavaria/Regierung von Mittelfranken).

### Alcohol drinking and alcohol deprivation effect

Alcohol drinking was tested in naive EFhd2 KO and WT mice using a two-bottle free-choice drinking paradigm. Animals were single housed for 3 month. Each cage was equipped with two bottles constantly available, one of which contained tap water and the other bottle contained alcohol in various concentrations. Bottle positions were changed daily. After an acclimatization period to establish a drinking baseline, animals received alcohol at increasing concentrations of 2, 4, 8, 12 and 16 vol. %. Mice were exposed to each concentration of alcohol for 4 days. Thereafter, alcohol concentration was maintained at 16 vol. % and animals were allowed to drink for 15 days. To measure the alcohol deprivation effect, alcohol was removed for 3 weeks (both bottles containing tap water) before it was re-introduced with a concentration of 16 vol. % for 4 days. This procedure was repeated once more. Bottles were changed and weighed daily. The consumed amount of alcohol relative to body weight and the preference vs water were measured.<sup>31,32</sup>

### Taste preference test

Alcohol experienced animals were used for this test 3 days after alcohol was replaced by water in the bottles. Sucrose (0.5 and 5%) and quinine (10 and 20 mg  $\text{dl}^{-1}$ ) preference vs water was measured in a two-bottle free-choice test, where one bottle contained either sucrose or quinine and the other always water. Each dose was offered for 3 days with the position of the bottles being changed and weighed daily.<sup>31,32</sup>

### Loss of righting reflex

Alcohol naive animals were used for this test. Animals were administered with an alcohol injection of 3.5 g  $\text{kg}^{-1}$  (intraperitoneal (i.p.);  $v_{inj} = 10 \text{ ml kg}^{-1}$ ) to induce a loss of the righting reflex (LORR), and immediately placed in an empty cage. A high dose was chosen for its known sedative effects in mice.<sup>32,33</sup> LORR was observed when the animal becomes ataxic and stopped moving for at least 30 s. The animal was then placed on its back. Recovery from alcohol administration was defined as the animal being able to right itself three times within a minute. A 2 h cutoff was used. Time taken for the animal to lose its righting reflex and time to recovery from alcohol's effect were recorded.<sup>32,33</sup>

### Blood alcohol determination

Alcohol naive animals were used for this test. Mice received alcohol injections with a dose of 3.0 g  $\text{kg}^{-1}$  (i.p.,  $v_{inj} = 10 \text{ ml kg}^{-1}$ ), which had no sedative effects and allowed for efficient blood sampling, and 20  $\mu\text{l}$  blood samples were obtained from the submandibular vein 1 and 2 h after alcohol injection. The blood samples were directly mixed with 80  $\mu\text{l}$  6.25% (w/v) trichloroacetic acid. After centrifugation, 15  $\mu\text{l}$  of the supernatant was subjected to enzymatic alcohol determination using the alcohol dehydrogenase method as described elsewhere.<sup>32,33</sup>

### Sensation-seeking and emotional behaviour

Naive EFhd2 KO and WT mice were tested through a battery of behavioural tests in the following order: open field, elevated plus maze (EPM), novelty-suppressed feeding, forced swim and sucrose preference tests. All tests were performed in separate days between 0900 and 1400 hours. Mice were tested in a pseudorandom order and were moved to the behavioural suite adjacent to the housing room immediately before testing. Each test apparatus was cleaned with 5% ethanol between subjects to avoid any olfactory cues influencing behaviours. Mice were returned to their home cages at the end of each test and allowed to recover for at least 5 days before further testing (for time line see: Supplementary Figure 1). Behaviours for all tests were recorded on videotape for subsequent scoring.<sup>34,35</sup>

**Open field.** Each mouse was placed in a square white acrylic arena (50 × 50 cm), facing an outer wall, for 20 min (parameters were measured per 5-min blocks and summarized) and allowed to freely explore the arena. White light of 25 lx was evenly distributed across the arena during testing. Video recordings were taken and analysed using Biobserve Viewer III (Biobserve, Bonn, Germany). A virtual square of equal distance from the periphery (36 × 36 cm) was defined as the 'central zone' to determine the number of entries and time (s) spent in the central zone. Distance moved in the outer and central zones (cm), number of entries, and time spent in the central zone were registered.<sup>34,35</sup>

**Elevated plus maze.** The EPM was constructed from black opaque acrylic with white lining on the floor, each arm measuring 30 × 5 cm and the central platform 5 × 5 cm. One set of arms, opposing one another, was enclosed completely by a wall of opaque acrylic, 15 cm high, whereas the other set was open with a ledge of 0.5 cm either side of the arms. The maze was elevated 50 cm from the ground on a transparent acrylic stand. Each mouse was placed on the central platform, facing towards a closed arm, and allowed to freely explore the maze for 5 min. Biobserve Viewer III tracking software (Biobserve) was used to record locomotor activity during the test (distance moved in the open and closed arms), and the number of entries into the closed and open arms and time spent in them. An arm entry was counted when two paws had entered an arm, and an arm exit was determined when two paws had left the arm.<sup>34,35</sup>

**Novelty-suppressed feeding.** Animals were deprived from food for 24 h before novelty-suppressed feeding test. After deprivation each mouse was put in the corner of a square white acrylic arena (50 × 50 × 50 cm), facing an outer wall. White light of 25 lx was evenly distributed across the arena during testing. A piece of food (standard food for mice; Sniff, Soest, Germany; ~5 g) was placed in the centre of the arena. Video recordings were taken and analysed using Biobserve Viewer III (Biobserve). The time (s) before a mouse began eating after the fasting period (24 h) and the distance moved before eating were registered. The cutoff time, which no animal reached, was 20 min.<sup>34,35</sup>

**Forced swim test.** For the forced swim test, each mouse was placed into a glass transparent cylinder (17-cm diameter, 18-cm height) filled with water (12 cm, 25 °C) for 15 min. Then, an animal was returned to the home cage. After 24 h, mice were again placed in this cylinder with water for 5 min. The latency of first floating and total floating time were recorded manually.<sup>34,35</sup>

**Sucrose preference test.** Animals were single housed and had access to two bottles with water 7 days before the sucrose preference test. At day 8, water in one bottle was replaced by 2% sucrose solution, and the position of bottles with water and sucrose solution was changed daily during the next 5 days. The weight of animals was measured before and after the test, and volume of water and sucrose solution was estimated daily. Sucrose preference in % of drunken fluid during baseline and testing was calculated.

### Reversal of enhanced alcohol consumption

We tested whether a pharmacological treatment that reverses the sensation-seeking/low-anxiety phenotype of EFhd2 KO mice would also reduce their alcohol consumption. To enhance anxiety-related behaviour, we used a chronic treatment with the well-established anxiogenic inverse benzodiazepine receptor agonist,  $\beta$ -carboline-3-carboxylate ethyl ester ( $\beta$ -CCE; Sigma-Aldrich, Darmstadt, Germany) or vehicle (dimethylsulphoxide:saline, 80:20)<sup>36</sup> applied by constant delivery by osmotic minipump to avoid the stress of chronic injections. Treatment allocation to the EFhd2 KO and WT mice was done randomly by drawing animal numbers. In a pretest, we determined a minipump delivery procedure based on previous protocols<sup>37</sup> and a dose of  $\beta$ -CCE, which was low enough to be anxiogenic in EFhd2 KO mice but without effect in WT mice. This was used for further testing. Naive EFhd2 and WT mice were deeply anaesthetised with isoflurane inhalation narcosis. In addition, 0.01 ml Rimadyl (5 mg kg<sup>-1</sup> Carprofen) analgesia was given subcutaneously (s.c.). Animals are implanted with an osmotic minipump (ALZET Model 2006; Charles River, Sulzfeld, Germany) into the back, administering  $\beta$ -CCE (1.5 mg kg<sup>-1</sup> per day; s.c.) for 42 days. After surgery, animals were single housed for 42 days in standard macrolone cages (type III) with two bottles available, each containing tap water. Eight to nine days after the start of the chronic  $\beta$ -CCE treatment, animals were tested for anxiety-related behaviour in the

EPM as described above. Four days later, alcohol drinking was tested in a free-choice two-bottle drinking paradigm with increasing doses of alcohol (2–16 vol. %) in one bottle, as described above. One day after testing, animals were killed and full delivery of minipump content was verified.

### Conditioned place preference

The establishment of conditioned place preference (CPP) was tested in naive EFhd2 KO and WT mice. The TSE Place Preference test boxes (TSE Systems, Bad Homburg, Germany) were made of non-transparent polyvinyl chloride with standard inside dimensions of 40 cm (L) × 15 cm (W) × 20 cm (H). The apparatus was divided into three fully automated compartments; the outer chambers measured 17 cm in length and the centre chamber 6 cm. The floor of the left chamber (compartment A) was covered with a smooth black rubber mat. The floor of the right chamber (compartment B) was covered with a patterned black rubber mat. The centre chamber was not covered and coloured white (compartment C). Activity was recorded in each compartment using high-resolution infrared sensors. The system automatically recorded the number of entries made, the sojourn time and distance moved in each compartment for each trial. An unbiased design was used, that is, half the mice were conditioned to their preferred compartment, and half to their non-preferred compartment.<sup>38</sup> Animals were injected (i.p.) immediately before each trial with either saline or 2 g kg<sup>-1</sup> alcohol (i.p.), a dose that has no sedative effects and that was previously shown to have efficient reinforcing effects in WT mice.<sup>38,39</sup> Mice were immediately transferred to the testing suite and placed into the CPP boxes, signifying the beginning of the trial period. The experiment involved four phases; habituation trial (one session), baseline testing (B1), conditioning trials (14 sessions) and preference tests (3 sessions, T1–T3). Trials were performed once daily.

**Habituation.** The habituation session was intended to acclimatize mice to the test procedure and apparatus prior to commencing the experiment. Mice were injected with saline and introduced into the centre compartment with free access to all three compartments for 20 min.

**Baseline test.** The pretest was designed to establish a baseline level of preference for each individual animal. Mice were conditioned to either their preferred or non-preferred compartment using a counterbalanced experimental design. Mice were injected with saline and introduced into the centre compartment with free access to all three compartments for 20 min.

**Conditioning trials.** Conditioning trials were performed in pairs; odd numbered pairings were conditioned with alcohol and even numbered pairings were conditioned with saline, this was balanced across groups. All animals received seven pairings with saline and seven pairings with alcohol. Mice were injected with either saline or an ethanol solution and introduced into one of two compartments, with restricted access, for 5 min.

**Preference tests.** To monitor the time course of CPP establishment, preference tests were systematically performed after one, three and seven conditioning trials. Before each test, mice were injected with saline and introduced into the centre compartment with free access to all three compartments for 20 min.<sup>38</sup>

### In vivo microdialysis

Naive EFhd2 and WT mice were deeply anaesthetised with an i.p. injection using a mixture of 4.12 ml saline (NaCl), 0.38 ml Ketaset (containing 100 mg ml<sup>-1</sup> ketamine) and 0.5 ml Domitor (containing 1 mg ml<sup>-1</sup> medetomidine hydrochloride) administered at 0.1 ml per 10 g body weight. In addition 0.01 ml Rimadyl (5 mg kg<sup>-1</sup> Carprofen) analgesia was given s.c. The animal was placed in a Kopf stereotaxic frame. Two guide cannulas (Microbiotech/se, Stockholm, Sweden) were aimed at the prefrontal cortex (PFC; A: +1.9; L: ± 0.8; V: -1.3 angle ± 10° from midline) and the nucleus accumbens (Nac; A: +1.2; L: ± 1.6; V: -4.3 angle ± 10° from midline) using coordinates relative to bregma,<sup>40,41</sup> and fixed in place using two anchor screws (stainless steel, d = 1.4 mm) and dental cement. Thereafter, animals were kept warm and allowed to recover from the anaesthetic. Animals were then returned to their home cages and monitored daily, allowing at least 5 days for complete recovery.

On the day of the experiment, microdialysis probes with membrane lengths of 2 mm for the PFC (MAB 6.14.2.) and 1 mm (MAB 6.14.1.) for the

Nac were inserted into the guide cannulae under a short (3–5 min) isoflurane anaesthesia and perfused with artificial cerebrospinal fluid (containing  $\text{Na}^+$  147 mmol,  $\text{K}^+$  4 mmol,  $\text{Ca}^{2+}$  2.2 mmol,  $\text{Cl}^-$  156 mmol,  $\text{pH}=7.4$ ). After probe insertion, the animal was placed into an open field ( $21 \times 21 \times 30$  cm). Water was provided *ad libitum* and room temperature maintained between 19 and 22 °C. Samples were collected every 20 min. Three samples were taken as baseline and the neurotransmitters dopamine (DA), serotonin and noradrenaline were quantified by high pressure liquid chromatography with electrochemical detection as described previously.<sup>40,41</sup> An injection of 2 g  $\text{kg}^{-1}$  alcohol, a non-sedative dose known to have reinforcing properties and to drive monoaminergic responses *in vivo*,<sup>31,32</sup> was then administered *i.p.* and further eight samples were collected. Once microdialysis experiments were completed, animals were killed by cervical dislocation. Brains were collected and probe localization was verified. Only mice with correct probe placement within the Nac and PFC according to Franklin and Paxinos<sup>42</sup> mouse brain atlas were considered for further analysis.

Microdialysis samples were analysed by high pressure liquid chromatography with electrochemical detection. The column was an ET 125/2, Nucleosil 120-5, C-18 reversed phase column (Macherey–Nagel, Düren, Germany) perfused with a mobile phase composed of 75 mM  $\text{NaH}_2\text{PO}_4$ , 4 mM KCl, 20  $\mu\text{M}$  ethylenediamine tetraacetic acid, 1.5 mM sodium dodecyl sulfate, 100  $\mu\text{l l}^{-1}$  diethylamine, 12% methanol and 12% acetonitrile adjusted to  $\text{pH}$  6.0 using phosphoric acid. The electrochemical detector (Intro, Antec, Leyden, The Netherlands) was set at 500 mV vs an *in situ* Ag/AgCl reference electrode (Antec) at 30 °C. This setup allows the simultaneous measurement of DA, serotonin and noradrenaline. The detection limit of the assay was 0.1 pg for all neurotransmitters with a signal–noise ratio of 2:1. Neurochemical data were not corrected for recovery.<sup>40,41</sup>

#### RNA isolation and quantitative PCR

After the alcohol drinking study (experiment I) and a parallel study with a cohort of mice that received only water in two bottles at the same time, mice were killed by cervical dislocation and brains were immediately collected and frozen on dry ice. Areas of interest were cut from coronal sections of 1-mm thickness according to anatomical coordinates taken from the Franklin and Paxinos<sup>42</sup> mouse brain atlas. In a preliminary analysis of EFhd2 expression in the mouse brain, we found the PFC as the area with highest messenger RNA expression (Supplementary Figure 2). Accordingly, total RNA from the PFC was isolated with RNeasy Mini kit (Qiagen, Hilden, Germany) according to the manufacturers' instructions. Tissue was mechanically homogenized in the lysis buffer using a TissueLyser LT bead mill and stainless steel beads (Qiagen). Isolated RNA was dissolved in RNase-free water and stored at  $-80$  °C. RNA quality and quantity were assessed on a Nanodrop ND-1000 UV-Vis spectrophotometer (NanoDrop Technologies, Rockland, DE, USA). RNA quality and quantity were assessed with an Agilent 2100 Bioanalyzer (Agilent Technologies, Santa Clara, CA, USA) and a Nanodrop ND-1000 UV-Vis spectrophotometer (NanoDrop Technologies). Biotin-labelled complementary RNA was obtained using the two-cycle eukaryotic target labelling assay and hybridized to Affymetrix GeneChip Mouse Genome 430 2.0 arrays according to the standard protocol (Affymetrix, Santa Clara, CA, USA). GeneChip Operating Software (Affymetrix) was used for quality controls of the assays and included scaling factor and percentage of genes present. Raw data from gene expression arrays (CEL files) were processed in Partek Genomics Suite, version 6.5 (Partek, St Louis, MO, USA) using GC-RMA algorithm normalization, principle components analysis without outliers and analysis of variance yielding *P*-values and fold change values.

For quantitative PCR with reverse transcription, 0.5  $\mu\text{g}$  of RNA was reverse-transcribed into complementary DNA (cDNA) using SuperScript VILO cDNA synthesis kit (Life Technologies, Darmstadt, Germany) according to the manufacturer's instructions. After completion and termination of the reverse transcription reaction, cDNA was diluted with 90  $\mu\text{l}$  LowTE and stored at  $-20$  °C. Quantitative real-time PCR was conducted on a LightCycler 480 real-time PCR system (Roche, Mannheim, Germany) using SYBR-green chemistry. Each quantitative PCR reaction contained 5  $\mu\text{l}$  FastStart Essential DNA Green Master (Roche), 1  $\mu\text{M}$  of each of two gene-specific primers and 2.5  $\mu\text{l}$  diluted cDNA (corresponding to 12.5 ng RNA) in a total volume of 10  $\mu\text{l}$ . Temperature profile used was: 95 °C for 5 min followed by 45 cycles of amplification (95 °C for 10 s, 60 °C for 20 s and 72 °C for 30 s) and by melting curve analysis. After run, PCR product specificity was assessed by the inspection of single peak melting curves. Threshold cycles (Ct) were determined with the second derivative maximum method using the LightCycler 480 software (release 1.5.0), and

relative messenger RNA expression levels were calculated in Microsoft Excel (Microsoft, Redmond, WA, USA) using the  $2^{-\Delta\Delta\text{Ct}}$  method.<sup>43</sup> Gene-specific PCR primers for differentially expressed candidate genes were retrieved from PrimerBank (<https://pga.mgh.harvard.edu/primerbank>). *Gusb* and *Hprt* were used as reference genes. Primer sequences can be found in Supplementary Table 7.

#### Mouse gene expression microarray analysis

We extracted the raw probe-level data from Affymetrix Mouse 430 version 2.0 CEL files and used the robust multi-array average algorithm for background correction, normalization and summarization of expression at probeset levels.<sup>44</sup> Probesets that are 'absent' (present/absent call using MASS) in all samples were filtered out from the analysis. We mapped each probeset to Entrez GeneID using Bioconductor annotation package.<sup>45</sup> We selected the probeset with the highest mean expression value in a particular data set when multiple probesets were mapped to the same GeneID.

#### Gene co-expression network analysis and module characterization

Network analysis was performed with weighted gene co-expression network analysis as previously described.<sup>46</sup> Briefly, we created a correlation matrix containing all pair-wise Pearson correlations between all genes across all samples. We then transformed the correlation matrix into a signed adjacency matrix using a power function with parameter  $\beta$ . The components of this matrix (connection strengths) were then used to calculate 'topological overlap', a robust and biologically meaningful measurement of gene similarity based on two genes' co-expression relationships with all other genes in the network. Finally, modules of highly correlated genes were determined using average linkage hierarchical clustering followed dynamic tree-cut algorithm. For this data set, we selected 5000 high variable genes and used the smallest  $\beta$  ( $=12$ ) that leads to an approximately scale-free network with the truncated scale-free fitting index  $R^2 > 0.9$ . Once modules were identified, each module was represented by the module eigengene (ME), defined as the first principal component of a module, and is the component that explains the maximum possible variability for all genes in a module. The ME is commonly used as a representative value for a module. We calculated Pearson correlations between each gene and each ME—referred to as a gene's module membership—along with the corresponding *P*-values.

Modules were characterized in two ways. First, ME of each module was tested for its association with phenotypic traits (genotype: EFhd2 KO vs WT, treatment: alcohol vs saline and genotype  $\times$  treatment interaction). Second, modules were annotated with known gene ontologies (GOs) to understand the biological significance of the module. To annotate each module, we used GO functional enrichment analysis implementation from the weighted gene co-expression network package.

#### Genetic association in a human sample

Data from 1980 adolescent participants (960 males) were available for analyses. The mean age of participants was 14.4 years old (s.d. = 0.41). The participants were community recruited from eight sites in France, Germany, Ireland and the United Kingdom as part of the IMAGEN study. Approval was obtained from all local research ethics committees. Written consent was obtained from both the participant and their parent/guardian. A detailed account of recruitment and assessment methods has been previously described.<sup>47</sup> Alcohol consumption behaviour was measured using the European School Survey Project on Alcohol and Other Drugs.<sup>48</sup> Specifically, we explored lifetime drinking frequency and lifetime binge drinking frequency (defined as consumption of five or more drinks in a row). Anxiety sensitivity was measured using the mean response from the five anxiety sensitivity items of the Substance Use Risk Profile Scale,<sup>49</sup> with a higher mean score indicating greater anxiety sensitivity.

**Genotyping.** DNA purification and genotyping were performed by the Centre National de Génotypage in Paris. DNA was extracted from whole blood samples (~10 ml) preserved in BD Vacutainer ethylenediamine tetraacetic acid tubes (Becton, Dickinson and Company, Oxford, UK) using Genra Puregene Blood kit (QIAGEN, Valencia, CA, USA) according to the manufacturer's instructions. Genotype information was collected at 582 982 markers using the Illumina HumanHap610 Genotyping BeadChip (Illumina, San Diego, CA, USA) as part of a previous genome-wide association study.<sup>47</sup>

Single-nucleotide polymorphisms (SNPs) with call rates of  $< 98\%$ , minor allele frequency  $< 1\%$  or deviation from the Hardy–Weinberg equilibrium

( $P < 1.00 \times 10^{-4}$ ) were excluded from the analyses. Individuals with an ambiguous sex code, excessive missing genotypes (failure rate  $> 2\%$ ) and outlying heterozygosity (heterozygosity rate of 3 s.d.'s from the mean) were also excluded. Identity-by-state similarity was used to estimate cryptic relatedness for each pair of individuals using PLINK software.<sup>50</sup> Closely related individuals with identity by descent ( $> 0.1875$ ) were eliminated from the subsequent analysis. Population stratification for the genome-wide association study data was examined by principal component analysis using EIGENSTRAT software.<sup>51</sup> The four HapMap populations were used as reference groups in the principal component analysis and individuals with divergent ancestry (from CEU) were also excluded. The imputation protocols used MaCH<sup>52</sup> for haplotype phasing and minimac<sup>53</sup> for imputation. Imputed dosage values were kept in the analysis if the quality of the imputation was high ( $R^2 > 0.5$ ). Imputed common SNPs with minor allele frequency  $> 0.01$  within 5000 base pairs up- and downstream of *EFHD2* gene were included in the following analysis. Partial correlation analyses were conducted to investigate gene-wide associations between *EFHD2* common SNPs and phenotypes. Permutation test were used to control for multiple testing where it is necessary.

### Similarities between genetic contributions for different phenotypes

The genetic contributions of a particular phenotype were calculated as the regression coefficients, that is, commonly known as the beta value, of univariate analyses between the given phenotype and all given SNPs, that is, 105 common SNPs of *EFHD2* in this study. The similarity statistic between two phenotypes was then calculated as the correlation between the corresponding groups of beta values. Because the SNP information was identical in estimating both genetic contributions, the null distribution of this correlation, that is, the similarity, can only be established through a permutation analysis, that is, re-calculating the similarity statistics with SNP data having its individuals randomly permuted. A two-tailed  $P$ -value can then be assessed as the number of permutation iterations with a correlation having its absolute value larger than the absolute value of the observed similarity statistic. To measure the similarities between genetic contributions shares the same idea of commonly used polygenic analysis. However, instead of predicting one phenotype from the other's genetic contribution, we compare the similarity between both of their genetic contributions.

### Human magnetic resonance imaging

Full details of the magnetic resonance imaging (MRI) acquisition protocols and quality checks have been described previously.<sup>47</sup> Brain images were segmented with the FreeSurfer software package (<http://surfer.nmr.mgh.harvard.edu/>) and the entire cortex of each individual was inspected for inaccuracies. Individuals with major malformations of the cerebral cortex were excluded from further analysis. Out of 1909 images, we focused on 1136 individuals passed a stringent quality control. The mean of left and right thickness of superior frontal gyrus (SFG) was included in the following analysis as it was found to be related to drinking behaviour. The effect of MRI site was controlled by adding it as a nuisance covariate in all statistical analyses.

### Mouse MRI

A total of  $n = 16$  naive *EFhd2* KO and WT mice, 8–16 weeks old, age and sex-matched, were examined *ex vivo* in a dedicated small animal MRI scanner at 4.7 T (Biospec 47/40, Bruker, Ettlingen, Germany) using a standard mouse brain coil of the manufacturer (Bruker). For each animal, T1-weighted images (voxel size  $0.086 \times 0.086 \times 0.160 \text{ mm}^3$ ) of the brain were acquired to determine the volume of hippocampus, ventricles, PFC, sensorimotor cortex and olfactory bulb of each brain by Aycan Osirix Pro (aycan Digitalsysteme, Würzburg, Germany) in combination with a segmentation plugin (Version 1.0, Chimaera, Erlangen, Germany).

### *Xenopus laevis* embryos and *in situ* hybridizations

*Xenopus* embryos were generated and cultured according to general protocols and staged according to the normal table of Nieuwkoop and Faber.<sup>54</sup> All procedures were performed according to the German animal use and care law (Tierschutzgesetz) and approved by the local authorities and committees (animal care and housing approval: I/39/EE006, Veterinärämter Erlangen; German state administration Bavaria/Regierung von Mittelfranken). At eight-cell stage *Xenopus* embryos were injected unilaterally into one dorso-animal blastomere with 0.4 pmol of *EFhd2*

morpholino (5'-GCTCGTCTGAAGCCATAGAGGT-3') or an unrelated control morpholino. To trace the injected side, 200 pg of pCS2- $\beta$ -galactosidase DNA was co-injected. At stage 28, the embryos were fixed and  $\beta$ -galactosidase staining was carried out to identify the injected side. The indicated genes were detected by whole-mount *in situ* hybridizations as described by Harland.<sup>55</sup> To analyse the expression of *efhd2* in *Xenopus* brains of stage 40 tadpoles, fixed specimen were dissected and *in situ* hybridization was carried out as above.

### Cell morphology

Newborn mice were killed and primary cortical neurons (CNs) were isolated and cultured as previously described.<sup>23</sup> pSuper vectors containing *EFhd2* short hairpin RNA (shRNA) and scrambled shRNA as well as the *EFhd2*-GFP vector have been described before.<sup>56,57</sup> The scrambled shRNA and the shRNA directed against *EFhd2* were subcloned into pSuper-NeoGFP (50) via *HindIII* and *EcoRI* restriction sites. After 7 days in culture, CNs were transfected with mRFP- $\beta$ Actin together with shScramble, sh*EFhd2* or *EFhd2*-GFP using Lipofectamin 2000 (Invitrogen, Thermo Fisher Scientific, Pinneberg, Germany) and 48 h later fixed in 4% paraformaldehyde for 15 min at room temperature. Transfected CNs were analysed with a Zeiss Apotome 2 microscope (Zeiss, Jena, Germany). Data were quantified using NeuronJ (ImageJ, National Institute of Mental Health, Bethesda, MD, USA).

### Statistics

All quantitative data were expressed as mean  $\pm$  s.e.m. Data were analysed using analysis of variances (for repeated measures where appropriate) and by pre-planned comparisons using Fisher's least significant difference tests with Bonferroni correction when appropriate.<sup>58</sup> For single-group comparisons of normally distributed data,  $t$ -tests were used. Although sex differences are well known in alcoholism-related behaviours,<sup>59</sup> a routine screen in each experiment did not indicate sex differences in this study. Therefore, data were collapsed for analysis. The software SPSS 17.0 (IBM, Armonk, NY, USA), PLINK v1.07 (Cambridge, MA, USA) and Statistica 9 (Statsoft, Tulsa, OK, USA) were used. A significance level of  $P < 0.05$  was used.

## RESULTS

### *EFhd2* is required for alcohol drinking and escalation of consumption

To determine the role of *EFhd2* in spontaneous alcohol consumption, we measured alcohol drinking in a two-bottle free-choice paradigm in *EFhd2* KO and WT mice. We found that *EFhd2* KO mice drink significantly more alcohol (genotype:  $F_{1,95} = 21.87$ ,  $P < 0.0001$ ; Figure 1a) and prefer it more to water than WT mice (genotype:  $F_{1,95} = 4.44$ ,  $P < 0.038$ ; Figure 1b). After initial drinking establishment, animals were left undisturbed in cages with 16 vol. % alcohol solution freely available. Daily measurement of consumption showed that alcohol intake escalated spontaneously in *EFhd2* KO mice. This increase became statistically significant after 10 days of drinking (genotype:  $F_{1,19} = 25.75$ ,  $P < 0.0001$ ; day:  $F_{22,418} = 2.82$ ,  $P < 0.0001$ ; Figure 1c), whereas WT mice showed constant consumption. As there was no external event to which the escalation of consumption and preference can be attributed, it is suggested that *EFhd2* provides resilience to accumulating alcohol effects in the brain that sensitise for the reinforcing effects. When animals were withdrawn from alcohol drinking and then reinstated, they showed an alcohol deprivation effect, which becomes evident by a short increase in consumption over several days. This resembles the human situation in alcohol-dependent patients. We tested alcohol consumption after two withdrawal periods of 3 weeks each. Results showed an increase in alcohol consumption in the WT mice after first ( $P = 0.0108$ ) and second withdrawal ( $P < 0.0001$ ), most evident in the area under the curve (Figure 1d). In the already escalated *EFhd2* KO mice, no alcohol deprivation effect was observed, but consumption remained elevated compared to WT mice ( $P \leq 0.0001$ ; Figures 1c and d). This was confirmed

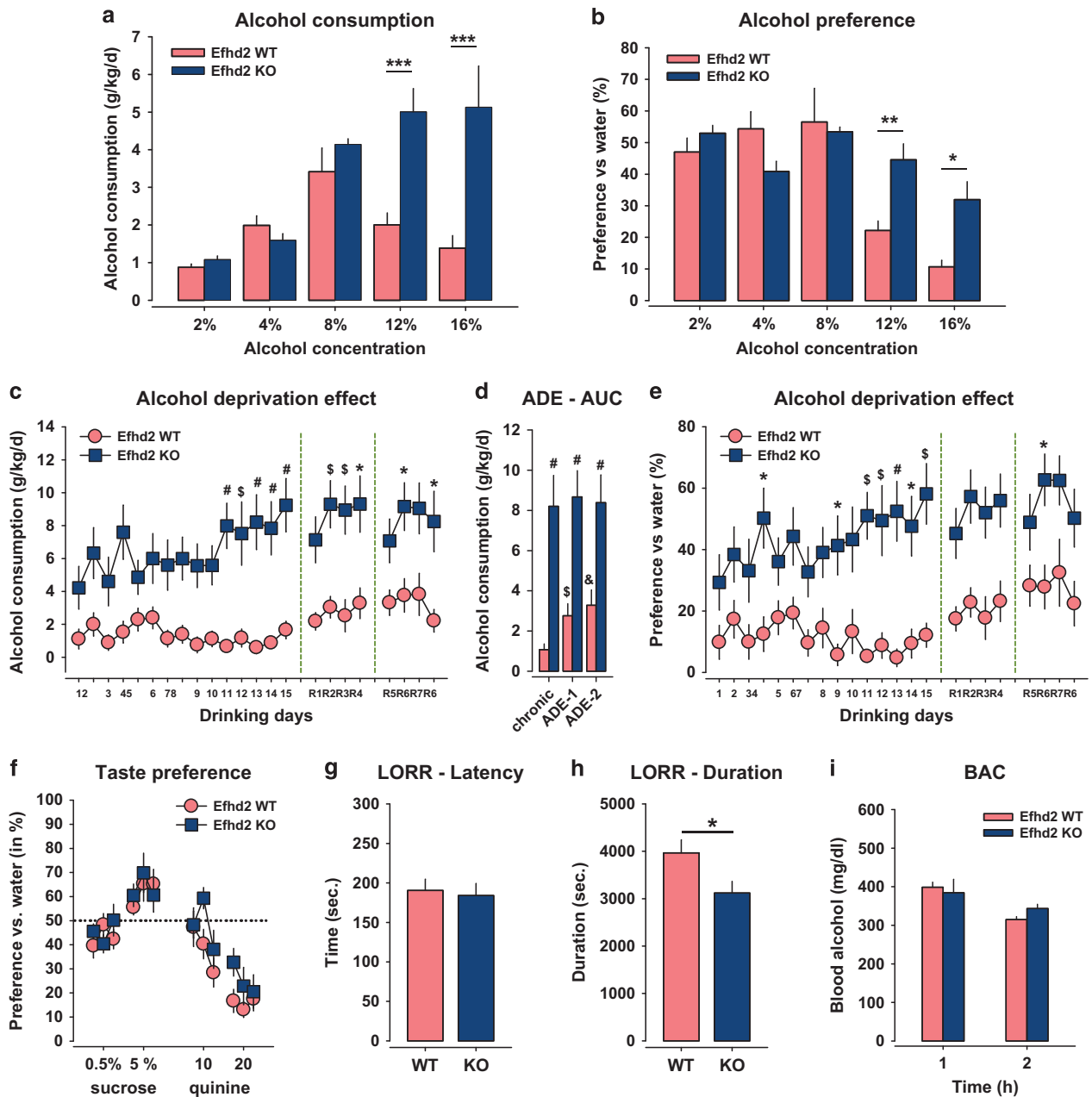


**Figure 1.** EFhd2 is a resilience factor for the establishment of alcohol drinking, the escalation of alcohol consumption and the sedating effects of alcohol. EFhd2 knockout (KO;  $n = 11$ ) and wild-type (WT;  $n = 10$ ) mice were tested in a free-choice two-bottle drinking paradigm for their alcohol consumption. (a) Amount of alcohol consumed at different concentrations of the drinking fluid. (b) Preference of alcohol versus water ( $*P < 0.05$ ,  $***P < 0.01$ ;  $***P < 0.001$ ). (c) Spontaneous escalation of 16 vol. % alcohol consumption after chronic drinking and alcohol deprivation effect (ADE) in EFhd2 KO ( $n = 11$ ) and WT ( $n = 10$ ) mice. After continuous drinking, animals were withdrawn from alcohol for 3 weeks (dotted lines) and reinstated for 4 days. (d) Average alcohol consumption as area under the curve (AUC) 4 days before and after withdrawal indicates an alcohol deprivation effect in WT mice, but not in EFhd2 KO mice ( $^{\$}P < 0.05$ ;  $^{\&}P < 0.001$  vs chronic consumption). (e) Spontaneous escalation in EFhd2 KO mice is confirmed in alcohol preference vs water ( $*P < 0.05$ ,  $^{\$}P < 0.01$ ;  $^{\#}P < 0.001$  vs WT). (f) Sucrose (sweet) preference and quinine (bitter) avoidance test in a free-choice two-bottle drinking paradigm indicates no difference between EFhd2 KO and WT mice in taste preference. EFhd2 KO mice show attenuated sedating effects of alcohol in the loss of righting reflex (LORR) test. (g) Latency to lose the righting reflex and (h) duration of sedation in EFhd2 KO ( $n = 19$ ) and WT ( $n = 23$ ) mice ( $*P < 0.05$ ). (i) Blood alcohol concentration in WT ( $n = 8$ ) and EFhd2 KO mice ( $n = 8$ ) after alcohol injection ( $3.0 \text{ g kg}^{-1}$ , intraperitoneal). Over the 2 h tested, there was no difference in alcohol bioavailability between genotypes ( $P > 0.05$ ).

by a spontaneous escalation of alcohol preference vs water in the EFhd2 KO mice (genotype:  $F_{1,19} = 23.68$ ,  $P < 0.0001$ ; day:  $F_{22,418} = 2.55$ ,  $P < 0.0002$ ; Figure 1e). It should be noted that the preference of 16 vol. % alcohol over water was initially  $< 50\%$ , but reached values of  $> 50\%$  during escalation in EFhd2 KO mice. This

may suggest that an initial aversive component was overcome by chronic alcohol exposure, a process that was accelerated in animals lacking EFhd2.

We further tested whether the lack of EFhd2 would lead to altered taste sensitivity in a taste preference test. Neither

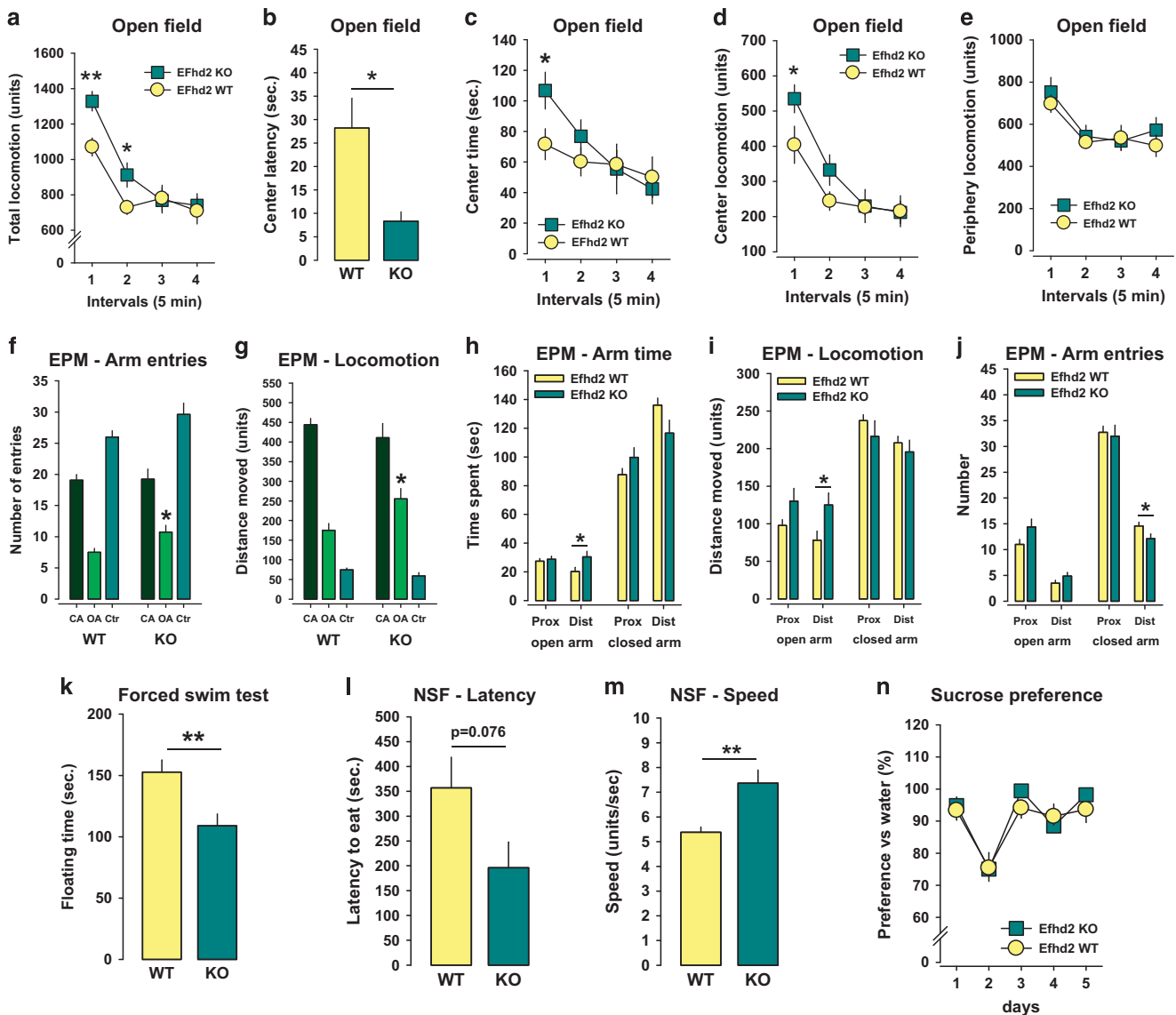


**Figure 2.** EFhd2 knockout (KO) mice display a sensation-seeking/low-anxiety behavioural phenotype that is frequently associated with an enhanced risk for alcohol addiction. (a) In the open-field (OF) test EFhd2 KO mice ( $n=9$ ) show higher locomotor activity in a novel environment than wild-type (WT) mice ( $n=12$ ). (b) The latency to enter the anxiogenic centre of the maze for the first time is reduced and (c) EFhd2 KO mice spend more time in the centre of the maze than WT mice. (d) Centre locomotion of EFhd2 KO mice is enhanced in the OF. (e) Locomotion in the periphery of the maze is not altered in EFhd2 KO mice. Also the elevated plus maze (EPM) test suggests reduced levels of anxiety in EFhd2 KO ( $n=8$ ) compared to WT ( $n=12$ ) mice. (f) The number of entries into the open arms is enhanced in EFhd2 KO mice. (g) Also, locomotion in the open arms is enhanced. In-depth analysis of anxiety-related behaviour in the EPM shows that major differences between EFhd2 KO and WT mice are derived from behaviour in most anxiety-loaded parts of the maze, that is, the distal part of the arms, as shown by (h) the time spent on proximal (Prox) and distal (Dist) arms of the maze, (i) the locomotor activity on all arms of the EPM, and by (j) the entries in the arms of the EPM. (k) In the forced swim test, EFhd2 KO mice show less immobility (floating) than WT mice. (l) The novelty-suppressed feeding (NSF) test shows a strong tendency for reduced depression-like behaviour in EFhd2 KO mice ( $n=8$ ) compared to WT ( $n=11$ ) mice. The latency to eat food in a novel environment is largely reduced in EFhd2 KO mice. (m) Speed of locomotion to search out for the food in the NSF test is significantly enhanced in EFhd2 KO mice, indicating a reduced suppression of feeding by the novelty of the environment. (n) The lack of EFhd2 has no effect on sucrose preference ( $*P < 0.05$ ;  $**P < 0.01$ ).

the preference for sweet tasting sucrose nor the avoidance of bitter tasting quinine solution was altered in EFhd2 KO mice compared to WT mice ( $P > 0.05$ ; Figure 1f). Although EFhd2 KO mice consumed significantly more alcohol over time, weight gain was comparable with WT mice (Supplementary Figure 3), suggesting that there was no overall increase in calorie intake in the EFhd2 KO mice compared to WT during alcohol drinking. This was supported by metabolic cage measurements without alcohol available, showing normal food and water

consumption in EFhd2 KO mice (Supplementary Figure 4). Altogether, these data show that EFhd2 is a negative regulator for alcohol preference and the control of alcohol consumption upon chronic exposure.

EFhd2 controls the sedating effects of alcohol

A high tolerance against the sedating effects of alcohol is a risk factor for the establishment of alcohol addiction in humans.

However, neuronal mechanisms of alcohol drinking and sedation frequently dissociate.<sup>33</sup> Therefore, we tested the sedating effect of alcohol in EFhd2 KO mice using the LORR test. The lack of EFhd2 had no effect on the latency of sedation after a high-dose alcohol injection ( $P > 0.05$ ; Figure 1g), but significantly reduced the duration of the sedating effects ( $t = -2.2637$ ,  $P = 0.0291$ ; Figure 1h). To rule out that altered bioavailability is a potential reason for the observed behavioural effects, we measured blood alcohol concentration (BAC) after a challenge dose in a new population of animals. Results showed that the lack of EFhd2 had no significant effect on alcohol BAC levels up to 2 h after administration ( $P > 0.05$ ; Figure 1i). Also after a high-dose alcohol ( $3.5 \text{ g kg}^{-1}$ , i.p.), as it was used for LORR, there was no difference in BAC between EFhd2 KO and WT mice at the time of LORR effects ( $P > 0.05$ ; Supplementary Figure 5). Altogether, these results suggest that EFhd2 enhances the sedating effects of alcohol, which may explain, in turn, the limiting effects on consumption.

#### EFhd2 deficiency leads to behavioural traits that are known addiction risk factors

In humans and animal models, particular personality traits are associated with an enhanced risk for the initiation of drug-seeking and consumption. These include enhanced sensation-seeking and low levels of trait anxiety.<sup>60–63</sup> Here we asked whether lack of EFhd2 function would result in a behavioural phenotype predictive for enhanced risk of alcohol addiction. A new group of animals was tested in the open-field test for novelty/sensation-seeking and anxiety-related behaviour.<sup>29,64</sup> EFhd2 KO mice showed significantly more total exploratory locomotion when exposed to a novel environment ( $P = 0.0067$  and  $P = 0.0499$ ; Figure 2a). There was a shorter latency to enter the centre ( $t = -2.6235$ ,  $P = 0.0167$ ), and EFhd2 KO mice spent significantly more time in the centre of a novel arena ( $P = 0.0364$ ) and showed more locomotion there ( $P = 0.0264$ ) than WT mice (Figures 2b–e). This trait was mainly limited to the first 5–10 min of exploration, suggesting that EFhd2 plays no role in novelty processing once stimulus habituation took place. EFhd2 KO mice were not more active than WT mice in the periphery of the maze ( $P > 0.05$ ; Figure 2e). These data suggest a novelty/sensation-seeking and low-anxiety trait in animals lacking EFhd2.

In the EPM test of anxiety, EFhd2 KO mice showed significantly more entries to the open arms ( $t = 2.7988$ ,  $P = 0.0118$ ) and more locomotion on these arms ( $t = 2.6553$ ,  $P = 0.0161$ ) compared to WT mice (Figures 2f and g). They also spent significantly more time on the most anxiety-associated distal part of the open arms ( $t = 2.1605$ ,  $P = 0.0444$ ; Figure 2h). They showed more locomotion in this part of the maze ( $t = 2.3823$ ,  $P = 0.0284$ ; Figure 2i), whereas entries to the distal closed arms were reduced ( $t = -2.1421$ ,  $P = 0.0461$ ; Figure 2j). Altogether, the EPM test suggests reduced trait anxiety in EFhd2 KO mice.

To further exclude a depression-like behaviour, we performed the forced swim test, which showed significantly reduced levels of floating in the EFhd2 KO mice ( $t = -3.1236$ ,  $P = 0.0053$ ; Figure 2k). In the novelty-suppressed feeding test of depression/anxiety-associated behaviour, a similar trend became obvious (Figure 2l). Interestingly, the speed of movement towards the food source was significantly enhanced in EFhd2 KO mice ( $t = 3.8908$ ,  $P = 0.0011$ ), supporting an enhanced activity in a novel environment (Figure 2m). We also measured the hedonic tone in EFhd2 KO mice using the sucrose preference test, where animals can choose in their consumption between a 2% sucrose solution and water. In this test, however, EFhd2 KO mice did not differ from WT mice ( $P > 0.05$ ; Figure 2n). Altogether, these findings suggest enhanced sensation-seeking and reduced anxiety-like behaviour in animals lacking EFhd2 in an aversive situation, but preserved hedonic processing in non-aversive situations. Overall, the behavioural characterization of EFhd2 KO mice suggests a

sensation-seeking/low-anxiety phenotype that is predictive for future alcohol misuse in adolescents<sup>62</sup> and associated with alcohol drinking and abuse in adults.<sup>61,63,65</sup>

#### Pharmacological reversal of low-anxiety state eliminates enhanced alcohol preference in EFhd2 KO mice

It has been suggested that personality traits such as sensation-seeking/low anxiety predispose individuals for an enhanced risk of alcohol misuse. We, therefore, asked whether a reversal of this trait would also reduce spontaneous alcohol consumption in EFhd2 KO mice. We treated a new group of animals sub-chronically for 35 days with either the anxiogenic compound  $\beta$ -CCE (1.5 mg kg per day) or with vehicle using osmotic minipumps (s.c.).<sup>36</sup> After 10 days of treatment, emotional behaviour and subsequently alcohol drinking was tested in a two-bottle free-choice drinking test. We found that  $\beta$ -CCE reversed low-anxiety levels of EFhd2 KO mice to the levels of WT animals in an EPM test (Figure 3a). Open arm ( $P = 0.0477$ ) and centre time ( $P = 0.0453$ ) were enhanced in EFhd2 KO mice vs WT when receiving vehicle treatment, but no longer, when  $\beta$ -CCE was administered ( $P > 0.05$ ). Correspondingly, closed arm time was reduced in EFhd2 KO mice ( $P = 0.026$ ) when receiving vehicle treatment, but no longer, when  $\beta$ -CCE was administered ( $P > 0.05$ ). Also locomotor activity on open arms was enhanced in EFhd2 KO mice as an indicator of sensation-seeking, which was reversed by  $\beta$ -CCE (Supplementary Figure 6). Subsequently, EFhd2 KO mice showed enhanced alcohol consumption (genotype:  $F_{1,140} = 17.081$ ,  $P < 0.0001$ ; dose:  $F_{4,140} = 253.568$ ,  $P < 0.0001$ ; interaction:  $F_{1,140} = 9.530$ ,  $P = 0.0024$ ), in particular, at doses of 12 vol. % ( $P = 0.0018$ ) and 16 vol. % alcohol ( $P = 0.0002$ ; Figure 3b). Alcohol consumption was normalized by  $\beta$ -CCE treatment in EFhd2 KO mice to the level of WT animals ( $P = 0.0147$  vs EFhd2 KO vehicle). In WT mice, the dose of  $\beta$ -CCE used here had neither an effect on emotional behaviour nor on alcohol consumption ( $P > 0.05$ ; Figures 3a and b). These findings suggest that EFhd2 deficiency is associated with a high-risk personality trait that leads to increased alcohol drinking.

EFhd2 has no role in the conditioned reinforcing effects of alcohol Drug addiction is a behavioural syndrome that is shaped by distinct learned behaviours.<sup>3,66</sup> One of them is the predominantly classically conditioned preference for places associated with alcohol action, as measured by CPP.<sup>67</sup> Given that EFhd2 is not uniformly expressed in the brain, a distinct involvement in different types of drug memories and addiction-related behaviours appeared very likely. Here we asked whether EFhd2 would also provide resilience to the establishment of conditioned reinforcing effects of alcohol. Using a two-compartment CPP box with seven conditioning and pseudo-conditioning trials and three tests to monitor the build-up of an alcohol CPP,<sup>38</sup> we found that alcohol i.p. injections induce a significant preference over time for the compartment paired with the drug (time:  $F_{3,90} = 3.112$ ,  $P = 0.030$ ; genotype:  $F_{1,30} = 0.228$ ,  $P = 0.637$ ; interaction:  $F_{3,90} = 0.272$ ,  $P = 0.845$ ). Entries into this compartment decreased significantly, suggesting an enhanced sojourn time after each visit. However, there was no significant difference in the time spent or entries to the conditioning compartment between EFhd2 KO and WT mice ( $P > 0.05$ ; Supplementary Figure 7). These findings suggest that EFhd2 does not provide resilience action to the establishment of the conditioned reinforcing effects of alcohol.

#### EFhd2 controls the mesolimbic, but not the mesocortical DA response

There are several motives for alcohol consumption in humans,<sup>3</sup> and distinct ways of how drinking may escalate from them.<sup>4</sup> A crucial mechanism is related to the pharmacological reinforcing effects of the alcohol, which is mediated by an activation of the



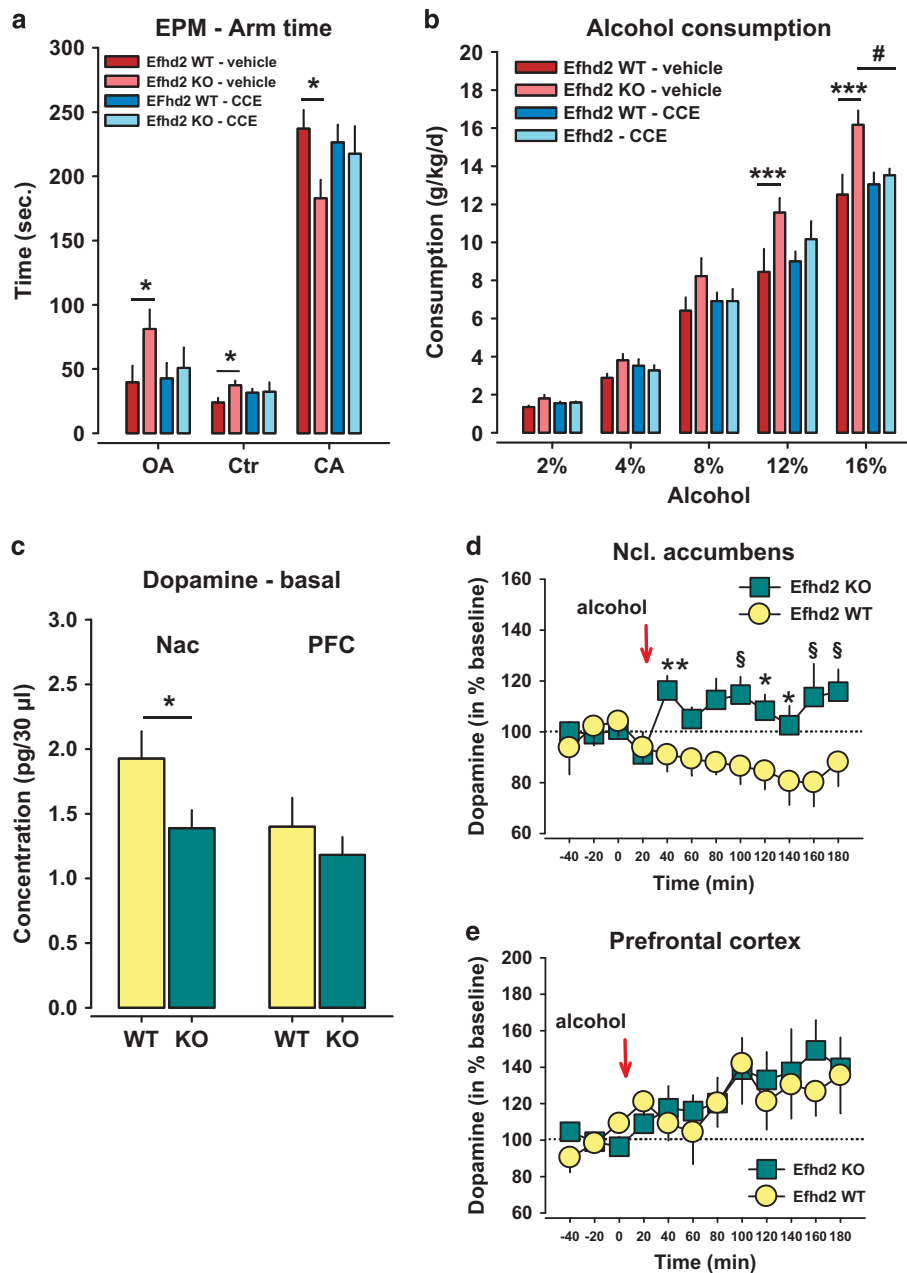


**Figure 3.** Low anxiety and high alcohol consumption in EFhd2 knockout (KO) mice can be reversed by chronic subcutaneous (s.c.) treatment with the anxiogenic drug  $\beta$ -carboline-3-carboxylate ethyl ester ( $\beta$ -CCE).  $\beta$ -CCE was administered s.c. by osmotic minipumps at a rate of  $1.5 \text{ mg kg}^{-1}$  per day. After 8–9 days of administration, the elevated plus maze (EPM) test revealed a reversal of the low-anxiety phenotype of EFhd2 KO mice ( $n = 7$  per group) to the level of wild-type (WT,  $n = 8$  and  $9$  per group) animals. **(a)** Time spent in the open (OA) and closed arm (CA) or centre (Ctr) of the EPM ( $*P < 0.05$ ). **(b)** Alcohol consumption in a two-bottle free-choice drinking paradigm in mice with chronic treatment with  $\beta$ -CCE or vehicle ( $***P < 0.001$ ;  $^{\#}P < 0.05$ ). **(c)** Dopamine basal levels in the nucleus accumbens (Nac) and prefrontal cortex (PFC) prior to alcohol treatment. EFhd2 is required for basal dopaminergic tone in the Nac, but not in the PFC of mice ( $*P < 0.05$ ). **(d)** EFhd2 limits the alcohol-induced increase in extracellular dopamine levels in the Nac, but not in the PFC of mice. Extracellular dopamine levels after acute alcohol ( $2 \text{ g kg}^{-1}$ , intraperitoneal) treatment in EFhd2 KO ( $n = 9$ ) and WT ( $n = 9$ ) mice in **(d)** the Nac and **(e)** PFC ( $*P < 0.05$ ,  $^{\S}P < 0.01$  vs WT).

mesocorticolimbic DA systems.<sup>68</sup> To characterize how EFhd2 provides resilience against alcohol drinking escalation, we measured alcohol-induced DA responses in target regions of the mesolimbic and mesocortical DA systems using *in vivo* microdialysis in freely moving animals.<sup>31,32</sup> We found that basal DA levels were significantly attenuated in the Nac ( $P < 0.0393$ ), but not in the PFC ( $P > 0.05$ ) of EFhd2 KO mice (Figure 3c). In the Nac, extracellular DA levels were significantly higher after a  $2 \text{ g kg}^{-1}$  (i.p.) alcohol injection in EFhd2 KO mice than in WT starting 20 min after

injection and persisting for up to 140 min (genotype:  $F_{1,16} = 8.344$ ,  $P < 0.0107$ ; Figure 3d). No difference in the DA increase after alcohol injection was observed in the PFC ( $P > 0.05$ ; Figure 3e). EFhd2 has an inhibitory effect on basal noradrenergic activity in the Nac as well as in the PFC, but has no role in serotonergic tone in these brain regions (Supplementary Figure 8). These findings suggest that EFhd2 might exert its resilience effects by enhancing basal DA levels and restricting alcohol-induced DA responses specifically in the mesolimbic, but not the mesocortical DA system.

### EFhd2 regulates gene expression after alcohol exposition

To investigate the molecular basis for the *Efhd2*-related differences in the alcohol response, we extracted RNA from PFC of mice which had been drinking alcohol or water for 3 months and performed genome-wide transcriptional analysis. The PFC was chosen as a brain area exerting important top-down cortical control on alcohol drinking.<sup>59</sup> Using two-way analysis of variance (genotype  $\times$  treatment), we identified 853 differentially expressed genes ( $P < 0.05$ ) for genotype, 1276 for treatment and 700 for the interaction. We next applied weighted gene co-expression network analysis to identify groups of genes (modules) with similar expression and identified 16 modules containing each 103–618 genes (labelled with arbitrary colour; Figure 4 and Table 1). Of these 16 modules, 2 were significantly associated with genotype (turquoise and green yellow) and four with treatment (pink, purple, tan and yellow), considering a false discovery rate of 0.05 (Table 1; Supplementary Figures 9 and 10). None of the modules satisfied this criterion for interaction.

All genes in the turquoise module were downregulated in *EFhd2* KO mice in comparison to WT, whereas the genes in the green-yellow module were upregulated (Figures 4e and f). To explore the biological relevance of the modules, we determined enrichment of GO terms. GO terms enriched in the turquoise module (618 genes) included developmental process, cell surface receptor signalling pathway, DA biosynthetic process and forebrain neuronal differentiation (Supplementary Table 1). We further performed pathway analysis and identified genes in the turquoise module involved in axon guidance, chemokine signalling, glutamatergic synapse, focal adhesion, ECM receptor interaction and long-term potentiation (Table 2). Importantly, the turquoise module includes *EFhd2* itself, strongly suggesting that the genes assigned to this module may have important biological relationships with *EFhd2*. The top differentially expressed genes in this module included *S100a5* ( $\log_2$  fold change,  $FC = -2.02$ ,  $P = 3.24 \times 10^{-06}$ ), which is known to bind  $Ca^{2+}$ ,<sup>69</sup> *Doc2g* ( $\log_2$   $FC = -1.71$ ,  $P = 1.22 \times 10^{-05}$ ), which is likely involved in vesicular trafficking,<sup>70</sup> *Th* ( $\log_2$   $FC = -1.31$ ,  $P = 1.14 \times 10^{-05}$ ), which has been implicated in DA synthesis and alcoholism,<sup>71</sup> and *Eomes* ( $\log_2$   $FC = -1.01$ ,  $P = 2.27 \times 10^{-04}$ ), which has been shown to be important for cortex development downstream of *Pax6*.<sup>72,73</sup> Of note, *Pax6* was also downregulated in *EFhd2* KO ( $\log_2$   $FC = -0.247$ ,  $P = 0.018$ ). The top differentially expressed genes of the turquoise module were all corroborated by quantitative PCR (Supplementary Figure 10). The green-yellow module consisted of 172 genes that were enriched for metal ion transport ( $P = 6.36 \times 10^{-05}$ ), chemical homeostasis ( $P = 8.56 \times 10^{-05}$ ), positive regulation of fatty acid transport ( $P = 9.81 \times 10^{-05}$ ), channel activity ( $P = 2.40 \times 10^{-04}$ ) and calcium ion homeostasis ( $P = 7.48 \times 10^{-04}$ ; Supplementary Table 2). Genes represented in the green-yellow module are involved in MAPK signalling, focal adhesion and mTOR signalling (Table 2). The alcohol-responsive modules also showed significant correlations between module membership and gene significance to the treatment effect (Supplementary Figure 9).

A majority of genes in the yellow module were upregulated by alcohol compared to water consumption, whereas all the genes in the three modules, tan, pink and purple, were downregulated (Supplementary Figure 10). GO term enrichment in the yellow module (537 genes) included cellular carbohydrate metabolic process, response to chemical stimuli, dendritic spine growth and acute inflammatory response (Supplementary Table 3). Pathway analysis revealed that genes included in the yellow module and upregulated in response to alcohol consumption are involved in chemokine, PPAR, calcium, JAK/STAT and phosphatidylinositol signalling as well as in long-term potentiation and glutamatergic synapses (Table 3). GO term enrichment included DA transport and regulation of neuronal apoptotic processes in the tan module (170 genes) (Supplementary Table 4), regulation of the MAPK

cascade, integrin activation and regulation of cell cycle in the pink module (295 genes; Supplementary Table 5), and regulation of phosphoprotein phosphatase activity, magnesium ion binding and regulation of mesenchymal cell proliferation in the purple module (192 genes) (Supplementary Table 6). Genes included in these modules and downregulated by alcohol consumption were found to be involved in the MAPK signalling pathway, tight junction, cell cycle and axon guidance (Table 3).

### *EFhd2*-controlled gene expression is associated with cortical maturation in mice and *Xenopus*

Two GO terms enriched in the *EFhd2*-controlled turquoise module were developmental processes and forebrain neuronal differentiation. Strikingly, *EFhd2* controlled the expression of genes associated with cortical maturation, *Eomes/Tbr2* and *Pax6*.<sup>72,73</sup> *Pax6* elicits normal development of cortical basal progenitor cells via *Eomes* expression<sup>74,75</sup> and cortical connections are shaped via the *Pax6*–*Eomes*–*Tbr1* axis.<sup>76</sup> *Pax6* mutations have been linked to progressive decline in thickness of the fronto-parietal cortex and cortex-dependent working memory with age in humans.<sup>74</sup> A specific role of *EFhd2* in the human cortex was previously suggested by Borger et al.<sup>22</sup> and the *Efhd2* gene is evolutionary conserved from *Drosophila* to *Xenopus* to humans.<sup>16</sup> We wished to translate our findings into the human situation. To test first for a principal evolutionary conservation of the *EFhd2* pathway and to confirm our gene expression data in a completely independent system, we analysed the effect of morpholino-mediated *EFhd2* downregulation in *Xenopus* tadpoles as an established model system. This would also provide an independent confirmation of our results obtained in mice. The expression of *Efhd2* was detected ubiquitously in the brain of *Xenopus laevis* stage 40 tadpoles.<sup>77</sup> In accordance with the expression of *Efhd2* in murine and human cortex,<sup>22,23</sup> we detected *Efhd2* messenger RNA also in the cortex of developing *Xenopus* tadpoles (Figure 5a). Enhanced *Efhd2* expression was also detected in the metencephalon, the ventral telencephalon and ventral diencephalon as well as in the pituitary primordia and at rhombomere borders in the hindbrain (Figure 5a). *Pax6*, is strongly expressed in the telencephalon and the eyes of early tadpoles.<sup>72,78</sup> Unilateral antisense morpholino oligonucleotide (Mo)-mediated knockdown of *EFhd2* resulted in a strong reduction of *Pax6* in the telencephalon, but not in the eye. A control morpholino did not affect *Pax6* expression (Figure 5b). Importantly, knockdown of *EFhd2* by morpholinos reduced *Pax6* expression in the forebrain, but not in the eye in over 90% of the *EFhd2* morpholino-injected embryos ( $n = 60$ ). In contrast, only 10% of the control morpholino-injected embryos show a reduction of *Pax6* on the injected side ( $n = 60$ ). At stage 28, *Eomes* is only expressed in the forebrain (Supplementary Figure 12), marked also by *Pax6* here, and in accordance, knockdown of *EFhd2* reduced *Eomes* expression (Figure 5c). Hence, regulation of *Pax6*/*Eomes* expression by *EFhd2* is evolutionary conserved between mouse and *Xenopus*. On the basis of these findings, we hypothesized that *EFhd2* might be involved in cortical development. To test for a role of *EFhd2* in cortical development, we investigated the morphological size of the PFC, the sensorimotor cortex, the hippocampus, the olfactory bulb and the ventricle size in *EFhd2* KO mice using MRI (Supplementary Figure 13). We observed that the volumes of the PFC ( $t = -2.5171$ ,  $P = 0.0246$ ) and sensorimotor cortex ( $t = -2.3911$ ,  $P = 0.031$ ), but not those of hippocampus, olfactory bulb or ventricles ( $P > 0.05$ ) were significantly reduced in *EFhd2* KO mice (Figure 5d). These data may provide a developmental mechanism for the high alcohol preference in *Efhd2* KO mice since reduced cortical maturation is associated with early onset of alcohol consumption in humans.<sup>79</sup>

### *EFhd2* controls neuronal morphology

Drug and alcohol exposition induces morphological plasticity at the level of neuronal spines and dendrites, which is supposed to

underlie the learning of drug-seeking and consumption behaviour.<sup>80,81</sup> Recent data suggested that EFhd2 might be involved in dendritic plasticity by regulating actin dynamics.<sup>21</sup>

Therefore, we used overexpression and shRNA-mediated knock-down of EFhd2 in murine primary CNs to investigate number and length of dendrites. We found that downregulation of EFhd2 led

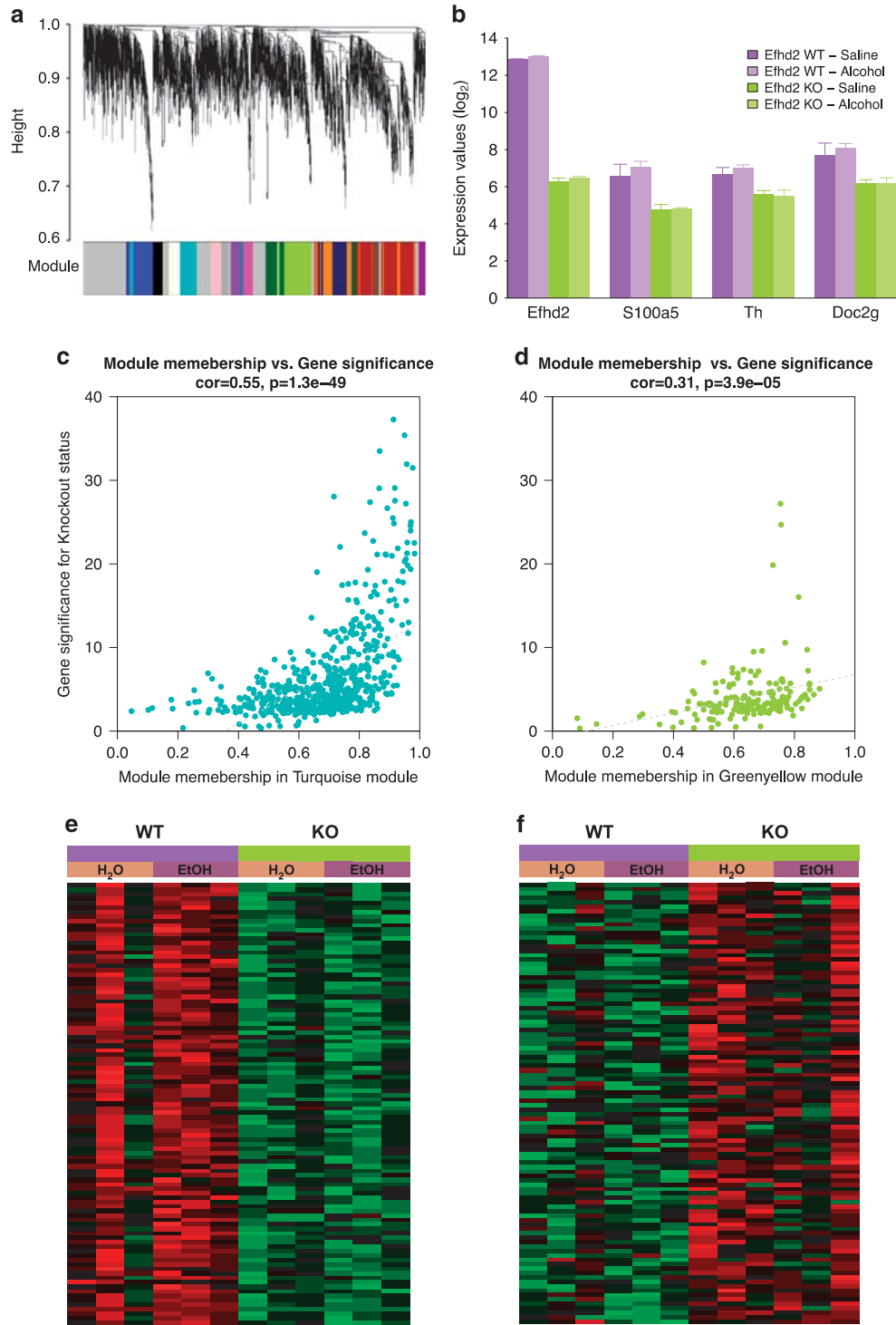


**Figure 4.** EFhd2 controls gene co-expression in the prefrontal cortex (PFC) of mice, a brain region with naturally high EFhd2 expression. **(a)** Weighted gene co-expression network analysis of mouse PFC expression data comparing alcohol or water drinking EFhd2 knockout (KO) and wild-type (WT) mice ( $n = 4$  PER group). Cluster dendrogram generated by hierarchical clustering of genes on the basis of topological overlap. Modules of correlated genes were assigned colours and are indicated by the horizontal bar beneath the dendrogram, where all unassigned genes were placed in the grey module. **(b)** Expression changes between WT and EFhd2 KO for selected candidate genes (EFhd2, S100a5, Th and Doc2g) of the turquoise model. **(c, d)** Scatter plot of correlations between gene significance (GS), that is, differential expression between WT and EFhd2 KO (F-statistics from the analysis of variance model) and module membership (MM) for turquoise and green-yellow modules. **(e, f)** Heatmap of top 100 genes in turquoise and green-yellow modules. In the heatmap, red represents high expression, whereas green represents low expression values.

**Table 1.** Summary of module characterization and phenotype association

Module	Module size		Genotype		Treatment		Interaction		Gene ontology enrichment		
	F	P	F	P	F	P	F	P	Category	N	P
Black	300	0.042	2.63	0.144	1.17	0.312	1.17	0.312	Response to organic substance (BP)	41	2.34E-04
Blue	566	0.246	7.46	0.026	0.93	0.362	0.93	0.362	Somitogenesis (BP)	9	9.41E-06
Brown	546	0.185	10.49	0.012	1.31	0.285	1.31	0.285	Negative regulation of JNK cascade (BP)	5	4.65E-04
Cyan	147	0.065	9.12	0.017	1.84	0.212	1.84	0.212	Oxidoreductase activity, acting on NAD(P)H, haem protein as acceptor (MF)	3	6.27E-05
Green	477	0.032	2.29	0.169	2.96	0.123	2.96	0.123	Multicellular organismal development (BP)	125	5.15E-11
Green yellow	172	0.005	1.11	0.323	0.00	0.981	0.00	0.981	Positive regulation of icosanoid secretion (BP)	3	4.64E-05
Light cyan	103	0.380	11.18	0.010	3.39	0.103	3.39	0.103	Extracellular region part (CC)	16	1.30E-05
Magenta	263	0.014	1.32	0.283	0.80	0.397	0.80	0.397	Tricarboxylic acid cycle (BP)	5	5.78E-05
Midnightblue	126	0.079	8.09	0.022	2.98	0.123	2.98	0.123	Negative regulation of cartilage development (BP)	2	1.75E-04
Pink	295	0.910	14.96	0.005	0.43	0.532	0.43	0.532	Positive regulation of interleukin-13 biosynthetic process (BP)	2	4.00E-04
Purple	192	0.564	13.09	0.007	0.54	0.485	0.54	0.485	Negative regulation of peptidyl-threonine phosphorylation (BP)	2	3.85E-03
Red	330	0.331	6.99	0.030	0.60	0.460	0.60	0.460	GTPase regulator activity (MF)	17	1.28E-03
Salmon	167	0.00	8.78	0.018	0.30	0.599	0.30	0.599	Rhythmic process (BP)	7	3.60E-04
Tan	170	0.227	23.07	0.001	5.87	0.042	5.87	0.042	Melanin biosynthetic process from tyrosine (BP)edede	2	1.19E-04
Turquoise	618	0.002	0.08	0.778	0.83	0.389	0.83	0.389	Extracellular region (CC)	84	7.47E-09
Yellow	537	0.705	11.98	0.009	0.02	0.885	0.02	0.885	Enzyme binding (MF)	67	6.56E-06

Abbreviations: BP, biological process; CC, cellular compartment; MF, molecular function. CC, MF and BP are the three ontologies used to classify GO terms.

to an increased number of secondary and tertiary dendrites (spines; Figures 6a and b). However, dendritic length was not altered (Figures 6c–e). Overexpression of *EFhd2* increased the number of tertiary dendrites and the length of secondary dendrites and spines (Figure 6). These findings suggest that *EFhd2* works at the micro-morphological level by controlling the number of neuronal dendrites.

*EFhd2* provides a link between trait anxiety and alcohol consumption in an adolescent human population

To translate our findings from animal models to humans, we investigated the link between naturally occurring genetic variations in the *EFhd2*-coding gene, as SNPs, with alcohol consumption behaviour from European School Survey Project on Alcohol and Other Drugs<sup>48</sup> ( $N=1773$ ) and anxiety traits from the Substance Use Risk Profile Scale<sup>49</sup> ( $N=1810$ ) in adolescents of the IMAGEN sample. In the IMAGEN sample, there are 105 imputed SNPs with minor allele frequency  $>0.01$  within the region ( $\pm 5000$  base pairs) of *EFhd2*. Of all these 105 SNPs, the minor C allele of rs112146896 (minor allele frequency = 2%) shows a positive significant association with the lifetime drinking frequency ( $r=0.099$ ,  $P=3.04 \times 10^{-5}$ ,  $P_{corrected}=2.08 \times 10^{-3}$  based on 100,000 permutations,  $df=1763$ ; Supplementary Figures 14 and 15A; Supplementary Table 8) and a nominal significant association with lifetime 5-binge drinking ( $r=0.055$ ,  $P=2.10 \times 10^{-2}$ ,  $df=1763$ ; Supplementary Figure 15B). Interestingly, an association in opposite direction was found for the minor C allele of SNP rs112146896 with anxiety sensitivity ( $r=-0.067$ ,  $P=4.16 \times 10^{-3}$ ,  $df=1800$ , Supplementary Figure 15C). In line with animal observations, these findings suggest that naturally occurring genetic variations in the *EFhd2*-coding gene may render human individuals both less anxiety sensitive and more prone to alcohol consumption.

To investigate whether the role of *EFhd2* in cortical development and adult cortex size translates into the human condition, we analysed cortex MRI data from adolescents of the IMAGEN sample. Similar to the previous findings,<sup>82</sup> the thickness of SFG was found to be negatively associated with alcohol consumption in humans. We observed a negative association between lifetime 5-binge drinking and the thickness of SFG ( $r=-0.067$ ,  $P_{one-tailed}=1.34 \times 10^{-2}$ ,  $P_{corrected}=2.40 \times 10^{-2}$  based on 100,000 permutations;  $df=1083$ ; Supplementary Figure 16A) and a trend for lifetime drinking frequency ( $r=-0.042$ ,  $P_{one-tailed}=8.22 \times 10^{-2}$ ,  $df=1083$ ; Supplementary Figure 16B). Although we did not find any association between SNP rs112146896 and the thickness of SFG, collectively the 105 common SNPs show significant similarity between the genetic contributions to lifetime 5-binge drinking and the thickness of SFG ( $P=0.0153$  based on 10,000 permutation), but not so between the genetic contributions to lifetime drinking frequency and the thickness of SFG ( $P=0.801$  based on 10,000 permutation). Altogether, these findings further support a role of *EFhd2* in cortical maturation and the control of alcohol drinking.<sup>79</sup>

## DISCUSSION

Here we identified *EFhd2* as a common genetic determinant for high-risk personality traits sensation-seeking/low anxiety and the escalation of alcohol drinking. We show that the absence of *EFhd2* leads to a higher preference for alcohol in mice, which then facilitates the spontaneous escalation of consumption. The lack of *EFhd2* also reduces the sedative effects of alcohol, which may contribute to an enhanced consumption by diminished aversive effects. Reduced aversive effects of alcohol intake in association with low sedation and other aversive effects have so far mainly been examined with respect to serotonergic neurotransmission, in which indeed low aversive effects correlate with high alcohol intake.<sup>82,83</sup> *EFhd2* does not affect taste preference or alcohol

**Table 2.** Pathways enriched with EFhd2-dependent genes from two co-expression modules

Pathway	N	FDR	Genes
<i>Downregulated (Turquoise module)</i>			
Viral myocarditis	9	8.50E-04	<i>Casp8, Abl2, Myh1, Bid, Myh8, Casp3, Cd28, Myh7, Fyn</i>
Pathways in cancer	17	8.96E-04	<i>Casp8, Msh3, Hdac2, Fgf16, Fgf1, Wnt7a, Vegfb, Ret, Bid, Pparg, Casp3, Mitf, Cdkn1a, Igf1, Ralb, Itga3, Ctbp2</i>
Axon guidance	10	1.83E-03	<i>Ablim3, Ntn4, Sema3c, Ntn1, Ppp3cc, Eph3, Efn3, Fyn, Rasa1, Gnai3</i>
Chemokine signalling pathway	11	3.96E-03	<i>Ccr2, Vav3, Gng4, Adcy8, Cxcl13, Grk5, Tiam2, Ppbp, Rap1b, Ncf1, Gnai3</i>
Taurine and hypotaurine metabolism	3	1.33E-02	<i>Cdo1, Gad1, Gad2</i>
Glutamatergic synapse	8	1.49E-02	<i>Slc38a3, Pla2g4d, Gng4, Adcy8, Ppp3cc, Slc17a6, Grm4, Gnai3</i>
β-Alanine metabolism	4	1.55E-02	<i>Gad1, Abat, Gad2, Acadm</i>
p53 signalling pathway	6	1.57E-02	<i>Casp8, Chek2, Bid, Casp3, Cdkn1a, Igf1</i>
Focal adhesion	10	1.58E-02	<i>Spp1, Vegfb, Vav3, Vtn, Igf1, Tnc, Itga3, Ppp1cc, Rap1b, Fyn</i>
Tight junction	8	1.66E-02	<i>Myh1, Myh8, Yes1, Inadl, Myh7, Jam2, Vapa, Gnai3</i>
MAPK signalling pathway	12	1.66E-02	<i>Pla2g4d, Fgf16, Fgf1, Cacng4, Map3k1, Mapkapk2, Casp3, Ppp3cc, Rap1b, Cacng5, Rasa2, Rasa1</i>
Other glycan degradation	3	2.49E-02	<i>Fuca2, Aga, Glb1</i>
Dilated cardiomyopathy	6	2.61E-02	<i>Cacng4, Adcy8, Igf1, Myh7, Itga3, Cacng5</i>
ECM receptor interaction	6	2.68E-02	<i>Spp1, Vtn, Tnc, Itga3, Sdc2, Sdc1</i>
Apoptosis	6	2.74E-02	<i>Casp8, Ripk1, Bid, Casp3, Irak2, Ppp3cc</i>
Long-term potentiation	5	3.58E-02	<i>Adcy8, Rapgef3, Ppp3cc, Ppp1cc, Rap1b</i>
Melanoma	5	4.62E-02	<i>Fgf16, Fgf1, Mitf, Cdkn1a, Igf1</i>
<i>Upregulated (green-yellow module)</i>			
MAPK signalling pathway	10	2.79E-02	<i>Pdgfa, Gadd45b, Nr4a1, Dusp1, Ptpn5, Fos, Dusp5, Dusp6, Pla2g2d, Akt1</i>
Focal adhesion	8	4.07E-02	<i>Pdgfa, Pik3r5, Col11a1, Myl9, Col4a2, Pxn, Col6a2, Akt1</i>
mTOR signaling pathway	4	4.98E-02	<i>Pik3r5, Ulk1, Akt1, Tsc2</i>

Abbreviation: FDR, false discovery rate.

**Table 3.** Pathways enriched with ethanol-responsive genes from four co-expression modules

Pathway	N	FDR	Genes
<i>Upregulated genes (yellow module)</i>			
Lysine degradation	8	2.25E-07	<i>Ehmt2, Setdb1, Plod1, Tmlhe, Whsc111, Gcdh, Ogdh, Plod2</i>
Chemokine signalling pathway	13	6.72E-07	<i>Pik3r5, Arrb2, Prkcd, Mapk3, Stat5b, Gnb1, Arrb1, Vav2, Ptk2b, Ptk2, Akt1, Stat3, Stat1</i>
Natural killer-cell-mediated cytotoxicity	9	3.18E-05	<i>Pik3r5, Mapk3, H2-D1, Itgb2, Lcp2, Fcer1g, Icam1, Vav2, Ptk2b</i>
PPAR signalling pathway	7	7.99E-05	<i>Lpl, Rxra, Slc27a4, Acox1, Scd1, Slc27a1, Cpt1c</i>
Calcium signalling pathway	10	1.05E-04	<i>Phkg1, Itpkb, Pde1b, Phka2, Mylk3, Grm1, Phkg2, Ptk2b, Camk2b, Adra1b</i>
Glycerophospholipid metabolism	6	6.39E-04	<i>Chkb, Lpcat2, Agpat6, Pnpla6, Mboat7, Pla2g2d</i>
Inositol phosphate metabolism	5	8.91E-04	<i>Inpp11, Inpp5a, Itpkb, Inpp5k, Isyna1</i>
Jak-STAT signalling pathway	8	9.49E-04	<i>Osmr, Pik3r5, Il7, Stat5b, Akt1, Il10rb, Stat3, Stat1</i>
Long-term potentiation	5	1.73E-03	<i>Mapk3, Rps6ka1, Grm1, Camk2b, Gria1</i>
Phosphatidylinositol signalling system	5	3.03E-03	<i>Inpp11, Pik3r5, Inpp5a, Itpkb, Inpp5k</i>
mRNA surveillance pathway	5	5.18E-03	<i>Upf3b, Casc3, Smg6, Acin1, Upf1</i>
Glutamatergic synapse	6	5.66E-03	<i>Mapk3, Grm1, Gnb1, Pla2g2d, Dlg4, Gria1</i>
<i>Downregulated genes (tan, pink, and purple modules)</i>			
MAPK signalling pathway	17	8.26E-07	<i>Pdgfa, Fgf9, Map2k6, Gadd45b, Ptprr, Gadd45g, Nr4a1, Fgf5, Dusp1, Kras, Fos, Dusp5, Dusp6, Jun, Map3k14, Nras, Rras2</i>
Tight junction	10	3.97E-05	<i>Gnai1, Myl9, Ctnna2, Ppp2r2d, Myh2, Pard6b, Kras, Cask, Nras, Rras2</i>
Osteoclast differentiation	9	7.97E-05	<i>Nfkb1a, Fosb, Map2k6, Fosl2, Junb, Fos, Jun, Map3k14, Socs3</i>
Regulation of actin cytoskeleton	11	4.80E-04	<i>Pdgfa, Fgf9, Myl9, Itga1, Itgae, Fgf5, Kras, Pip5k1b, Arpc3, Nras, Rras2</i>
Cell cycle	8	6.51E-04	<i>Gadd45b, Gadd45g, Ccne2, Cdkn2c, Cdk6, Ccnb2, Ccnh, Ccna1</i>
B-cell receptor signalling pathway	6	1.05E-03	<i>Nfkb1a, Kras, Fos, Cd72, Jun, Nras</i>
Axon guidance	7	4.06E-03	<i>Efn2, Gnai1, Rnd1, Kras, Cxcl12, Met, Nras</i>

Abbreviations: ANOVA, analysis of variance; FDR, false discovery rate; GO, gene ontology; mRNA, messenger RNA. For each module, the table lists its size (number of genes), phenotypic association using the ANOVA model for the genotype, treatment and genotype × treatment interaction, GO term, number of genes from the module that are included in the listed GO term (N), and enrichment P-value. For each module, only the top term is listed.

bioavailability in mice. These findings translate to the human condition, where we found an association of SNP rs112146896 in the *EFhd2*-coding region with the amount of alcohol drinking in non-addicted adolescents. The emotional behaviour of mice lacking *EFhd2* is characterized by enhanced sensation-seeking and reduced anxiety in several tests. However, the consumption of a hedonic stimulus was not altered. This is in line with animal models of sensation-seeking showing a positive relationship

between the response to a novel environment and operant alcohol self-administration in rats.<sup>84</sup> There is a strong relationship between sensation-seeking and arousal.<sup>63,64</sup> In our study, *EFhd2* KO mice not only showed an enhanced response to a novel environment but also enhanced brain tissue NA levels, which suggests a higher baseline arousal level in *EFhd2* KO mice. Our findings are paralleled in a human sample, which also shows an association of *EFhd2* SNP rs112146896 with anxiety traits.

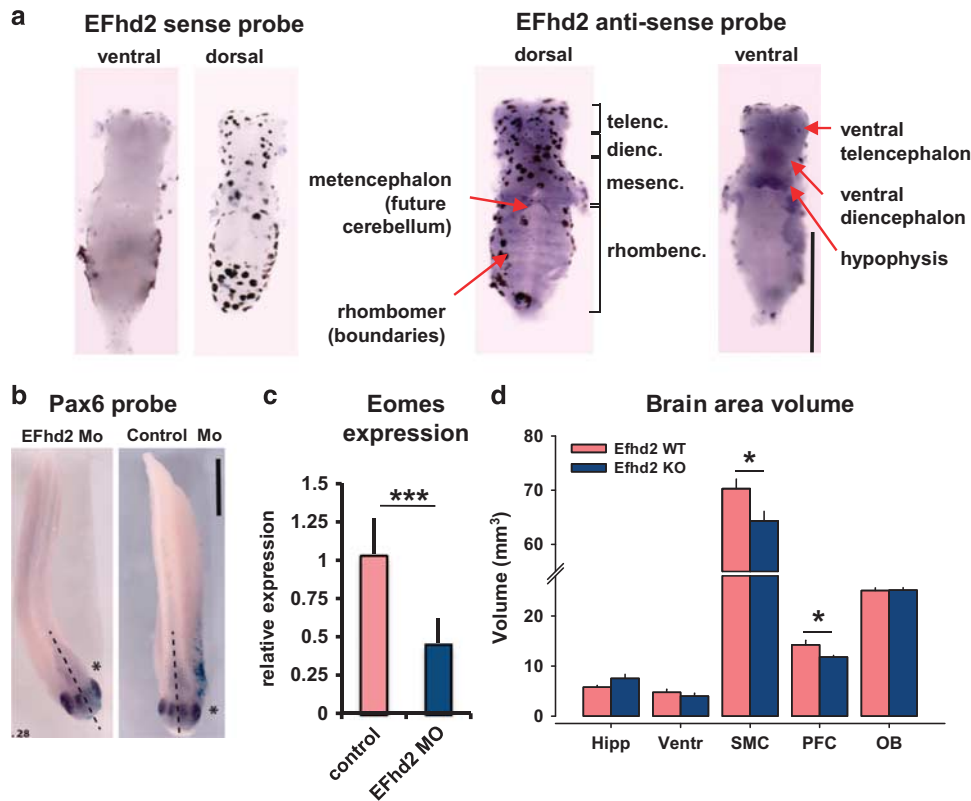


**Figure 5.** EFhd2 controls cortical development and micro-morphology of neuronal cells. **(a)** *In situ* hybridization against *Efh2* expression in explanted brains of *Xenopus* stage 40 tadpoles. A sense probe was used to identify unspecific binding (bar: 0.5 mm). **(b)** At the eight-cell stage, *Xenopus* embryos were injected unilaterally into one dorso-animal blastomere with EFhd2 morpholino or an unrelated control morpholino, along with a lacZ-encoding plasmid. The star (\*) marks the injected side. At stage 28,  $\beta$ -galactosidase activity was visualized to identify the injected side. Pax6 was detected by whole-mount *in situ* hybridization (bar: 1 mm). **(c)** At the eight-cell stage, *Xenopus* embryos were injected unilaterally into one dorso-animal blastomere with EFhd2 morpholino or an unrelated control morpholino. At stage 28, Eomes expression was assessed by quantitative PCR ( $***P < 0.001$ ). **(d)** Brain area volume of adult EFhd2 knockout (KO) and wild-type (WT) mice measured with magnetic resonance imaging. Hipp, hippocampus; OB, olfactory bulb; PFC, prefrontal cortex; SMC, sensorimotor cortex; Ventr, ventricle;  $*P < 0.05$ .

Enhanced sensation-seeking/low anxiety is associated with reduced impulse control and engagement in dangerous behaviour.<sup>61</sup> It is also uniquely associated with alcohol consumption through its tendency to expose individuals more frequently to alcohol as an 'enhancement' or as a 'stress-coping strategy'.<sup>3,62</sup> A limitation of this approach is that it cannot predict how rs112146896 affects the expression of EFhd2 in the human brain during development and adulthood. As behavioural associations and cortical morphology show a comparable pattern between EFhd2 KO mice and the human rs112146896 haplotype, it is likely that this haplotype is associated with reduced EFhd2 expression during development. Altogether, our findings suggest that the long-known association of high sensation-seeking/low-anxiety phenotype with enhanced alcohol drinking could be causally mediated by EFhd2.

The analysis of downstream consequences of reduced EFhd2 function in mice showed altered activity in monoaminergic systems. There was a reduced dopaminergic and enhanced noradrenergic tone in the Nac and enhanced noradrenergic activity in the Nac and PFC. Serotonin activity did not depend on EFhd2. Furthermore, EFhd2 appears to limit the DA response to an alcohol challenge in the Nac, but not in the PFC. This points to a dissociation of EFhd2 involvement in DA neurons of the mesolimbic vs the mesocortical system. Reduced basal DA level and enhanced Nac DA response to alcohol implies that the delta in DA activity after drug treatment, which determines the reward magnitude,<sup>85</sup> is much enhanced when EFhd2 is lacking. This is

consistent with the sensation-seeking phenotype<sup>12,86</sup> and with the enhanced consumption of alcohol in EFhd2 KO mice. It further supports the view that a common end path leading to enhanced drug preference in sensation-seeking individuals is the enhanced sensitivity of the dopaminergic system to pharmacological reward.<sup>29,87,88</sup> Altogether, the neurochemical endophenotype suggests that EFhd2 provides resilience to alcohol consumption by reducing DA activation-mediated reward magnitude of alcohol.

The establishment of drug-seeking and consumption involves numerous active learning processes,<sup>3,89</sup> which require synaptic plasticity.<sup>4,80,90</sup> In line, both downregulation as well as overexpression of EFhd2 in primary CNs increased dendrite and spine formation. The lack of EFhd2 may therefore contribute to a hyperplasticity at cellular level, which favours the fast establishment of those alcohol-related memories that are mediated by mesocortical monoamine systems as it was observed for other addictive drugs.<sup>80</sup> Accordingly, upstream from altered function of monoaminergic systems appeared a considerable number of genes that are differentially expressed in the PFC of EFhd2 KO mice. They included genes involved in developmental processes, cell surface receptor signalling pathways, DA biosynthetic processes and forebrain neuronal differentiation. These findings appear in line with altered basal DA levels on the one hand and reduced cortical development on the other hand. The latter was confirmed by the finding that EFhd2 is required for full cortical, but not hippocampal maturation, in mice. A reduced cortical volume was shown to be a strong predictor of future alcohol misuse in

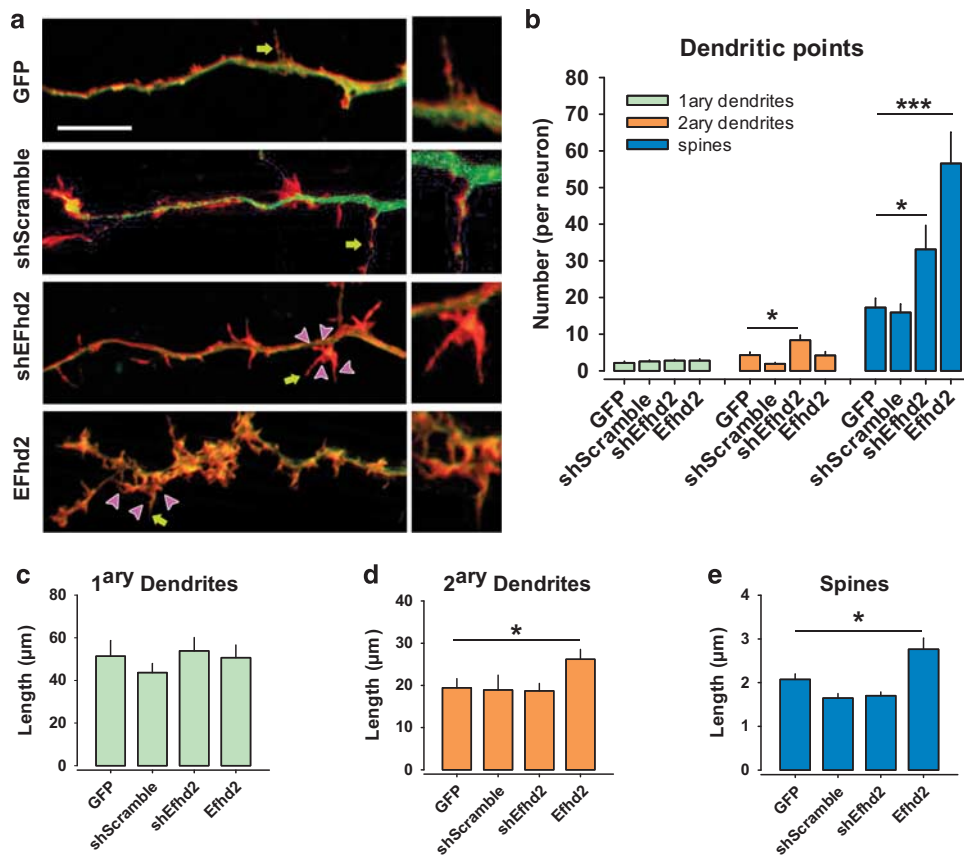


**Figure 6.** EFhd2 controls neuronal spine density and dendritic length. (a) Primary cortical neurons were transfected with short hairpin RNAs (shRNAs; scrambled or directed against EFhd2) linked to green fluorescent protein (GFP) expression, with GFP expressing or EFhd2-IRES-GFP vectors, fixed and stained with phalloidine-rhodamine. (b–e) Dendrites and spines of green cells were analysed with ImageJ. Data are shown as mean+s.e.m. (\* $P < 0.05$ ; \*\*\* $P < 0.001$ ).

adolescents,<sup>55</sup> and, thus, adds to the risk profile induced by reduced EFhd2 activity. This is most likely mediated by reduced cognitive impact on impulse control and drug-taking behaviour.<sup>12</sup> In how far an EFhd2 dysfunction and resulting cortical deficits contribute to symptoms of other psychiatric disorders such as, for example, schizophrenia has to be determined in future studies.

The mesocorticolimbic system constitutes a regulatory circuit involving the PFC, the Nac and the ventral tegmental area (VTA), whereby the PFC projects to the Nac and the VTA to control mesolimbic DA projections that modulate rewarding behaviour.<sup>91</sup> In support of a role of the PFC in the EFhd2-controlled rewarding response, EFhd2 was more expressed in the PFC than in Nac or VTA (Supplementary Figure 2). We found that a loss of EFhd2 can control transcriptional changes in the PFC, thereby controlling mesocorticolimbic projections. Alcohol consumption was associated with differential expression of several gene expression modules that include genes known to be crucial for the establishment of alcohol consumption, including genes involved in long-term potentiation and glutamatergic synapses.<sup>68,92</sup> However, there was very little interaction between EFhd2 and alcohol on gene expression profiles. We propose that EFhd2 controls gene expression in a way that controls behavioural traits and the risk of alcohol consumption initiation, but does not control the way how alcohol itself affects gene expression after consumption. This interpretation is in accordance with the reversal of the addictive phenotype by  $\beta$ -carboline. However, it does not exclude the possibility that gene expression after the loss of EFhd2 is not modulated in other areas of the brain such as the Nac or the VTA.

In conclusion, we identify that EFhd2/Swiprosin-1 is a common genetic determinant for sensation-seeking/low anxiety and alco-

hol addiction. We showed that a lack of EFhd2 induces high-risk personality traits associated with enhanced alcohol consumption. The resilience provided by EFhd2 and co-regulated genes may work by its control of monoamine basal activity and DA-mediated alcohol reward magnitude in the mesolimbic system of the brain on the one hand. On the other hand, EFhd2 and co-expressed genes are required for full cortical development and, thereby, indirectly control personality traits and alcohol consumption levels. These data would support preventive approaches using EFhd2 expression as a predictive marker during development and for therapeutic approaches in alcohol addiction treatment that enhance EFhd2 activity.

#### CONFLICT OF INTEREST

TB has served as an advisor or consultant to Bristol-Myers Squibb, Desitin Arzneimittel, Eli Lilly, Medice, Novartis, Pfizer, Shire, UCB and Vifor Pharma; he has received conference attendance support, conference support or speaking fees from Eli Lilly, Janssen McNeil, Medice, Novartis, Shire and UCB; and he is involved in clinical trials conducted by Eli Lilly, Novartis and Shire; the present work is unrelated to these relationships. JG has received research funding from the German Federal Ministry of Education and Research, AstraZeneca, Eli Lilly, Janssen-Cilag and Bristol-Myers Squibb; he has received speaking fees from AstraZeneca, Janssen-Cilag and Bristol-Myers Squibb. The remaining authors declare no conflict of interests.

#### ACKNOWLEDGMENTS

We thank Mr Benedikt Quinger for technical assistance. The present work was funded by the Interdisciplinary Center for Clinical Research (IZKF) Erlangen, Project E22, in part by Projects E8 and N3, and by the Deutsche Forschungsgemeinschaft grant DFG SCHA965/9-1. It was performed in partial fulfilment of the requirements for obtaining

the degree 'Dr med.' by Daniel Zilske, Elif Kirmizi-Alsan, Penelope Schönberger and Melissa Mettang. This work received further support from the following sources: the European Union-funded FP6 Integrated Project IMAGEN (Reinforcement-related behaviour in normal brain function and psychopathology; LSHM-CT- 2007-037286), the FP7 projects IMAGEMEND(602450; IMAGING GENetics for MENTAL Disorders), AGGRESSOTYPE (602805) and MATRICS (603016), the Innovative Medicine Initiative Project EU-AIMS (115300-2), the Medical Research Council Grants "Developmental pathways into adolescent substance abuse" (93558) and Consortium on Vulnerability to Externalizing Disorders and Addictions [c-VEDA] (MR/N000390/1), the Swedish funding agencies VR, FORTE and FORMAS, the Medical Research Council and the Wellcome Trust (Behavioural and Clinical Neuroscience Institute, University of Cambridge), the National Institute for Health Research (NIHR) Biomedical Research Centre at South London and Maudsley NHS Foundation Trust and King's College London, the Bundesministerium für Bildung und Forschung (BMBF grants 01GS08152; 01EV0711; eMED SysAlc01ZX1311A; 01GQ113; Forschungsnetz AERIAL), and the Deutsche Forschungsgemeinschaft (DFG grants SM 80/7-1, SM 80/7-2, SFB 940/1). Further support was provided by grants from: ANR (project AF12-NEUR0008-01 - WM2NA, and ANR-12-SAMA-0004), the Fondation de France, the Fondation pour la Recherche Médicale, the Mission Interministérielle de Lutte-contre-les-Drogues-et-les-Conduites-Addictives (MILDECA), the Assistance-Publique-Hôpitaux-de-Paris and INSERM (interface grant), Paris Sud University IDEX 2012; the National Institutes of Health, U.S.A. (Axon, Testosterone and Mental Health during Adolescence; RO1 MH085772-01A1), and by NIH Consortium grant U54 EB020403, supported by a cross-NIH alliance that funds Big Data to Knowledge Centres of Excellence. SB und JS were funded by the German Center for Cardiovascular Research (DZHK).

## REFERENCES

- Wittchen HU, Jacobi F, Rehm J, Gustavsson A, Svensson M, Jonsson B et al. The size and burden of mental disorders and other disorders of the brain in Europe 2010. *Eur Neuropsychopharmacol* 2011; **21**: 655–679.
- Ahmed SH. Toward an evolutionary basis for resilience to drug addiction. *Behav Brain Sci* 2011; **34**: 310–311.
- Müller CP, Schumann G. Drugs as instruments: a new framework for non-addictive psychoactive drug use. *Behav Brain Sci* 2011; **34**: 293–310.
- Müller CP, Homberg JR. The role of serotonin in drug use and addiction. *Behav Brain Res* 2015; **277C**: 146–192.
- Heath DB. *Drinking occasions: Comparative Perspectives on Alcohol and Culture*. Brunner/Mazel: Philadelphia, USA, 2000.
- Anderson P, Baumberg B. *Alcohol in Europe*. Institute of Alcohol Studies: London, UK, 2006.
- Wagner FA, Anthony JC. From first drug use to drug dependence; developmental periods of risk for dependence upon marijuana, cocaine, and alcohol. *Neuropsychopharmacology* 2002; **26**: 479–488.
- Chen CY, Anthony JC. Epidemiological estimates of risk in the process of becoming dependent upon cocaine: cocaine hydrochloride powder versus crack cocaine. *Psychopharmacology* 2004; **172**: 78–86.
- Heyman GM. Resolving the contradictions of addiction. *Behav Brain Sci* 1996; **19**: 561–610.
- SAMSHA. Results from the 2013 National Survey on Drug Use and Health: Summary of National Findings, Substance Abuse and Mental Health Services Administration, Rockville, MD, USA, 2014.
- Chen J, Repunte-Canonigo V, Kawamura T, Lefebvre C, Shin W, Howell LL et al. Hypothalamic proteoglycan syndecan-3 is a novel cocaine addiction resilience factor. *Nat Commun* 2013; **4**: 1955.
- Morrow JD, Flagel SB. Neuroscience of resilience and vulnerability for addiction medicine: From genes to behavior. *Prog Brain Res* 2016; **223**: 3–18.
- Maclaren EJ, Sikela JM. Cerebellar gene expression profiling and eQTL analysis in inbred mouse strains selected for ethanol sensitivity. *Alcohol Clin Exp Res* 2005; **29**: 1568–1579.
- Vuadens F, Rufer N, Kress A, Corthesy P, Schneider P, Tissot JD. Identification of swiprosin 1 in human lymphocytes. *Proteomics* 2004; **4**: 2216–2220.
- Kroczeck C, Lang C, Brachs S, Grohmann M, Dutting S, Schweizer A et al. Swiprosin-1/EFhd2 controls B cell receptor signaling through the assembly of the B cell receptor, Syk, and phospholipase C gamma2 in membrane rafts. *J Immunol* 2010; **184**: 3665–3676.
- Dutting S, Brachs S, Mielenz D. Fraternal twins: Swiprosin-1/EFhd2 and Swiprosin-2/EFhd1, two homologous EF-hand containing calcium binding adaptor proteins with distinct functions. *Cell Commun Signal* 2011; **9**: 2.
- Hagen S, Brachs S, Kroczeck C, Furnrohr BG, Lang C, Mielenz D. The B cell receptor-induced calcium flux involves a calcium mediated positive feedback loop. *Cell Calcium* 2012; **51**: 411–417.
- Gu J, Lee CW, Fan Y, Komlos D, Tang X, Sun C et al. ADF/cofilin-mediated actin dynamics regulate AMPA receptor trafficking during synaptic plasticity. *Nat Neurosci* 2010; **13**: 1208–1215.
- Huh YH, Kim SH, Chung KH, Oh S, Kwon MS, Choi HW et al. Swiprosin-1 modulates actin dynamics by regulating the F-actin accessibility to cofilin. *Cell Mol Life Sci* 2013; **70**: 4841–4854.
- Kwon MS, Park KR, Kim YD, Na BR, Kim HR, Choi HJ et al. Swiprosin-1 is a novel actin bundling protein that regulates cell spreading and migration. *PLoS ONE* 2013; **8**: e71626.
- Mielenz D, Gunn-Moore F. Physiological and pathophysiological functions of Swiprosin-1/EFhd2 in the nervous system. *Biochem J* 2016; **473**: 2429–2437.
- Borger E, Herrmann A, Mann DA, Spiers-Jones T, Gunn-Moore F. The calcium-binding protein EFhd2 modulates synapse formation in vitro and is linked to human dementia. *J Neuropathol Exp Neurol* 2014; **73**: 1166–1182.
- Purohit P, Perez-Branguli F, Prots I, Borger E, Gunn-Moore F, Welzel O et al. The Ca2+ sensor protein swiprosin-1/EFhd2 is present in neurites and involved in kinesin-mediated transport in neurons. *PLoS ONE* 2014; **9**: e103976.
- Vega IE, Traverso EE, Ferrer-Acosta Y, Matos E, Colon M, Gonzalez J et al. A novel calcium-binding protein is associated with tau proteins in tauopathy. *J Neurochem* 2008; **106**: 96–106.
- Ferrer-Acosta Y, Rodriguez-Cruz EN, Orange F, De Jesus-Cortes H, Madera B, Vaquer-Alicea J et al. EFhd2 is a novel amyloid protein associated with pathological tau in Alzheimer's disease. *J Neurochem* 2013; **125**: 921–931.
- Martins-de-Souza D, Gattaz WF, Schmitt A, Rewerts C, Maccarrone G, Dias-Neto E et al. Prefrontal cortex shotgun proteome analysis reveals altered calcium homeostasis and immune system imbalance in schizophrenia. *Eur Arch Psychiatry Clin Neurosci* 2009; **259**: 151–163.
- Zuckerman M. The psychobiological model for impulsive unsocialized sensation seeking: a comparative approach. *Neuropsychobiology* 1996; **34**: 125–129.
- Schwarting RK, Thiel CM, Müller CP, Huston JP. Relationship between anxiety and serotonin in the ventral striatum. *Neuroreport* 1998; **9**: 1025–1029.
- Norbury A, Husain M. Sensation-seeking: dopaminergic modulation and risk for psychopathology. *Behav Brain Res* 2015; **288**: 79–93.
- Brachs S, Turqueti-Neves A, Stein M, Reimer D, Brachvogel B, Bosl M et al. Swiprosin-1/EFhd2 limits germinal center responses and humoral type 2 immunity. *Eur J Immunol* 2014; **44**: 3206–3219.
- Stacey D, Bilbao A, Maroteaux M, Jia T, Easton AC, Longueville S et al. RASGRF2 regulates alcohol-induced reinforcement by influencing mesolimbic dopamine neuron activity and dopamine release. *Proc Natl Acad Sci USA* 2012; **109**: 21128–21133.
- Easton AC, Lucchesi W, Lourdasamy A, Lenz B, Solati J, Golub Y et al. alphaCaMKII autophosphorylation controls the establishment of alcohol drinking behavior. *Neuropsychopharmacology* 2013; **38**: 1636–1647.
- Zheng F, Puppel A, Huber SE, Link AS, Eulenburg V, van Brederode JF et al. Activin controls ethanol potentiation of inhibitory synaptic transmission through GABA receptors and concomitant behavioral sedation. *Neuropsychopharmacology* 2016; **41**: 2024–2033.
- Easton AC, Lucchesi W, Schumann G, Giese KP, Müller CP, Fernandes C. alpha-CaMKII autophosphorylation controls exploratory activity to threatening novel stimuli. *Neuropharmacology* 2011; **61**: 1424–1431.
- Süss P, Kalinichenko L, Baum W, Reichel M, Kornhuber J, Loskarn S et al. Hippocampal structure and function are maintained despite severe innate peripheral inflammation. *Brain Behav Immun* 2015; **49**: 156–170.
- Yeung M, Lu L, Hughes AM, Treit D, Dickson CT. FG7142, yohimbine, and betaCCe produce anxiogenic-like effects in the elevated plus-maze but do not affect brainstem activated hippocampal theta. *Neuropharmacology* 2013; **75**: 47–52.
- Amato D, Natesan S, Yavich L, Kapur S, Müller CP. Dynamic regulation of dopamine and serotonin responses to salient stimuli during chronic haloperidol treatment. *Int J Neuropsychopharmacol* 2011; **14**: 1327–1339.
- Easton AC, Lucchesi W, Mizuno K, Fernandes C, Schumann G, Giese KP et al. alphaCaMKII autophosphorylation controls the establishment of alcohol-induced conditioned place preference in mice. *Behav Brain Res* 2013; **252**: 72–76.
- Cunningham CL, Gremel CM, Groblewski PA. Drug-induced conditioned place preference and aversion in mice. *Nat Protoc* 2006; **1**: 1662–1670.
- Müller CP, De Souza Silva MA, Huston JP. Double dissociating effects of sensory stimulation and cocaine on serotonin activity in the occipital and temporal cortices. *Neuropharmacology* 2007; **52**: 854–862.
- Pum M, Carey RJ, Huston JP, Müller CP. Dissociating effects of cocaine and d-amphetamine on dopamine and serotonin in the perirhinal, entorhinal, and prefrontal cortex of freely moving rats. *Psychopharmacology* 2007; **193**: 375–390.
- Franklin KJB, Paxinos G. *The Mouse Brain in Stereotaxic Coordinates*. Academic Press: San Diego, USA, 1997.
- Livak KJ, Schmittgen TD. Analysis of relative gene expression data using real-time quantitative PCR and the 2(-Delta Delta C(T)) Method. *Methods* 2001; **25**: 402–408.
- Irizarry RA, Hobbs B, Collin F, Beazer-Barclay YD, Antonellis KJ, Scherf U et al. Exploration, normalization, and summaries of high density oligonucleotide array probe level data. *Biostatistics* 2003; **4**: 249–264.



- 45 Gentleman RC, Carey VJ, Bates DM, Bolstad B, Dettling M, Dudoit S et al. Bioconductor: open software development for computational biology and bioinformatics. *Genome Biol* 2004; **5**: R80.
- 46 Stacey D, Lourdasamy A, Ruggeri B, Maroteaux M, Jia T, Cattrell A et al. A translational systems biology approach in both animals and humans identifies a functionally related module of accumbal genes involved in the regulation of reward processing and binge drinking in males. *J Psychiatry Neurosci* 2015; **41**: 150138.
- 47 Schumann G, Loth E, Banaschewski T, Barbot A, Barker G, Büchel C et al. The IMAGEN study: reinforcement-related behaviour in normal brain function and psychopathology. *Mol Psychiatry* 2010; **15**: 1128–1139.
- 48 Morgan M, Hibell B, Andersson B, Bjarnason T, Kokkevi A, Narusk A. The ESPAD study: implications for prevention. *Drug Educ Prev Policy* 1999; **6**: 243–256.
- 49 Woicik PA, Stewart SH, Pihl RO, Conrod PJ. The Substance Use Risk Profile Scale: a scale measuring traits linked to reinforcement-specific substance use profiles. *Addict Behav* 2009; **34**: 1042–1055.
- 50 Purcell S, Neale B, Todd-Brown K, Thomas L, Ferreira MA, Bender D et al. PLINK: a tool set for whole-genome association and population-based linkage analyses. *Am J Hum Genet* 2007; **81**: 559–575.
- 51 Price AL, Patterson NJ, Plenge RM, Weinblatt ME, Shadick NA, Reich D. Principal components analysis corrects for stratification in genome-wide association studies. *Nat Genet* 2006; **38**: 904–909.
- 52 Li Y, Willer CJ, Ding J, Scheet P, Abecasis GR. MaCH: using sequence and genotype data to estimate haplotypes and unobserved genotypes. *Genet Epidemiol* 2010; **34**: 816–834.
- 53 Howie B, Fuchsberger C, Stephens M, Marchini J, Abecasis GR. Fast and accurate genotype imputation in genome-wide association studies through pre-phasing. *Nat Genet* 2012; **44**: 955–959.
- 54 Nieuwkoop PD, Faber J. External and internal stage criteria in the development of *Xenopus laevis*. Normal Tables of *Xenopus laevis*, 1975; 162–188.
- 55 Harland RM. In situ hybridization: an improved whole-mount method for *Xenopus* embryos. *Methods Cell Biol* 1991; **36**: 685–695.
- 56 Avramidou A, Kroczyk C, Lang C, Schuh W, Jack HM, Mielenz D. The novel adaptor protein Swiprosin-1 enhances BCR signals and contributes to BCR-induced apoptosis. *Cell Death Differ* 2007; **14**: 1936–1947.
- 57 Brummelkamp TR, Bernards R, Agami R. A system for stable expression of short interfering RNAs in mammalian cells. *Science* 2002; **296**: 550–553.
- 58 Ramsey PH. Multiple comparisons of independent means. In: Edwards LK (ed.). *Applied Analysis of Variance in Behavioral Science*. Marcel Dekker: New York, USA, 1993; p 25–61.
- 59 Lenz B, Müller CP, Stoessel C, Sperling W, Biermann T, Hillemecher T et al. Sex hormone activity in alcohol addiction: integrating organizational and activational effects. *Prog Neurobiol* 2012; **96**: 136–163.
- 60 Piazza PV, Deminiere JM, Le Moal M, Simon H. Factors that predict individual vulnerability to amphetamine self-administration. *Science* 1989; **245**: 1511–1513.
- 61 Stautz K, Cooper A. Impulsivity-related personality traits and adolescent alcohol use: a meta-analytic review. *Clin Psychol Rev* 2013; **33**: 574–592.
- 62 Whelan R, Watts R, Orr CA, Althoff RR, Artiges E, Banaschewski T et al. Neuro-psychosocial profiles of current and future adolescent alcohol misusers. *Nature* 2014; **512**: 185–189.
- 63 Peritogiannis V. Sensation/novelty seeking in psychotic disorders: a review of the literature. *World J Psychiatry* 2015; **5**: 79–87.
- 64 Blanchard MM, Mendelsohn D, Stamp JA. The HR/LR model: Further evidence as an animal model of sensation seeking. *Neurosci Biobehav Rev* 2009; **33**: 1145–1154.
- 65 Magid V, Maclean MG, Colder CR. Differentiating between sensation seeking and impulsivity through their mediated relations with alcohol use and problems. *Addict Behav* 2007; **32**: 2046–2061.
- 66 White NM. Addictive drugs as reinforcers: multiple partial actions on memory systems. *Addiction* 1996; **91**: 921–949.
- 67 Huston JP, Silva MA, Topic B, Müller CP. What's conditioned in conditioned place preference? *Trends Pharmacol Sci* 2013; **34**: 162–166.
- 68 Spanagel R. Alcoholism: a systems approach from molecular physiology to addictive behavior. *Physiol Rev* 2009; **89**: 649–705.
- 69 Streicher WW, Lopez MM, Makhatadze GI. Modulation of quaternary structure of S100 proteins by calcium ions. *Biophys Chem* 2010; **151**: 181–186.
- 70 Fukuda M, Mikoshiba K. Doc2gamma, a third isoform of double C2 protein, lacking calcium-dependent phospholipid binding activity. *Biochem Biophys Res Commun* 2000; **276**: 626–632.
- 71 Verheij MM, Cools AR. Twenty years of dopamine research: individual differences in the response of accumbal dopamine to environmental and pharmacological challenges. *Eur J Pharmacol* 2008; **585**: 228–244.
- 72 Sansom SN, Griffiths DS, Faedo A, Kleinjan DJ, Ruan Y, Smith J et al. The level of the transcription factor Pax6 is essential for controlling the balance between neural stem cell self-renewal and neurogenesis. *PLoS Genet* 2009; **5**: e1000511.
- 73 Sessa A, Mao CA, Colasante G, Nini A, Klein WH, Broccoli V. Tbr2-positive intermediate (basal) neuronal progenitors safeguard cerebral cortex expansion by controlling amplification of pallial glutamatergic neurons and attraction of sub-pallial GABAergic interneurons. *Genes Dev* 2010; **24**: 1816–1826.
- 74 Yogarajah M, Matarin M, Vollmar C, Thompson PJ, Duncan JS, Symms M et al. PAX6, brain structure and function in human adults: advanced MRI in aniridia. *Ann Clin Transl Neurol* 2016; **3**: 314–330.
- 75 Quinn JC, Molinek M, Martynoga BS, Zaki PA, Faedo A, Bulfone A et al. Pax6 controls cerebral cortical cell number by regulating exit from the cell cycle and specifies cortical cell identity by a cell autonomous mechanism. *Dev Biol* 2007; **302**: 50–65.
- 76 Elsen GE, Hodge RD, Bedogni F, Daza RA, Nelson BR, Shiba N et al. The protomap is propagated to cortical plate neurons through an Eomes-dependent intermediate map. *Proc Natl Acad Sci USA* 2013; **110**: 4081–4086.
- 77 Diaz-Alonso J, Aguado T, de Salas-Quiroga A, Ortega Z, Guzmán M, Galve-Roperh I. CB1 cannabinoid receptor-dependent activation of mTORC1/Pax6 signaling drives Tbr2 expression and basal progenitor expansion in the developing mouse cortex. *Cereb Cortex* 2015; **25**: 2395–2408.
- 78 Moreno N, Rétaux S, González A. Spatio-temporal expression of Pax6 in *Xenopus* forebrain. *Brain Res* 2008; **1239**: 92–99.
- 79 Wilson S, Malone SM, Thomas KM, Iacono WG. Adolescent drinking and brain morphometry: a co-twin control analysis. *Dev Cogn Neurosci* 2015; **16**: 130–138.
- 80 Robinson TE, Kolb B. Structural plasticity associated with exposure to drugs of abuse. *Neuropharmacology* 2004; **47**: 33–46.
- 81 Zhou FC, Anthony B, Dunn KW, Lindquist WB, Xu ZC, Deng P. Chronic alcohol drinking alters neuronal dendritic spines in the brain reward center nucleus accumbens. *Brain Res* 2007; **1134**: 148–161.
- 82 Heinz A, Higley JD, Gorey JG, Saunders RC, Jones DW, Hommer D et al. In vivo association between alcohol intoxication, aggression, and serotonin transporter availability in nonhuman primates. *Am J Psychiatry* 1998; **155**: 1023–1028.
- 83 Hinckers AS, Laucht M, Schmidt MH, Mann KF, Schumann G, Schuckit MA et al. Low level of response to alcohol as associated with serotonin transporter genotype and high alcohol intake in adolescents. *Biol Psychiatry* 2006; **60**: 282–287.
- 84 Nadal R, Armario A, Janak PH. Positive relationship between activity in a novel environment and operant ethanol self-administration in rats. *Psychopharmacology* 2002; **162**: 333–338.
- 85 Samaha AN, Robinson TE. Why does the rapid delivery of drugs to the brain promote addiction? *Trends Pharmacol Sci* 2005; **26**: 82–87.
- 86 Yau WY, Zubieta JK, Weiland BJ, Samudra PG, Zucker RA, Heitzeg MM. Nucleus accumbens response to incentive stimuli anticipation in children of alcoholics: relationships with precursive behavioural risk and lifetime alcohol use. *J Neurosci* 2012; **32**: 2544–2551.
- 87 Hooks MS, Colvin AC, Juncos JL, Justice J-BJ. Individual differences in basal and cocaine-stimulated extracellular dopamine in the nucleus accumbens using quantitative microdialysis. *Brain Res* 1992; **587**: 306–312.
- 88 Leyton M, Boileau I, Benkelfat C, Diksic M, Baker G, Dagher A. Amphetamine-induced increases in extracellular dopamine, drug wanting, and novelty seeking: a PET/[11C] raclopride study in healthy men. *Neuropsychopharmacology* 2002; **27**: 1027–1035.
- 89 Müller CP. Episodic memories and their relevance for psychoactive drug use and addiction. *Front Behav Neurosci* 2013; **7**: 34.
- 90 Zweifel LS, Argilli E, Bonci A, Palmiter RD. Role of NMDA receptors in dopamine neurons for plasticity and addictive behaviours. *Neuron* 2008; **59**: 486–496.
- 91 McBride WJ, Murphy JM, Ikemoto S. Localization of brain reinforcement mechanisms: intracranial self-administration and intracranial place-conditioning studies. *Behav Brain Res* 1999; **101**: 129–152.
- 92 Schumann G, Johann M, Frank J, Preuss U, Dahmen N, Laucht M et al. Systematic analysis of glutamatergic neurotransmission genes in alcohol dependence and adolescent risky drinking behavior. *Arch Gen Psychiatry* 2008; **65**: 826–838.



This work is licensed under a Creative Commons Attribution-NonCommercial-NoDerivs 4.0 International License. The images or other third party material in this article are included in the article's Creative Commons license, unless indicated otherwise in the credit line; if the material is not included under the Creative Commons license, users will need to obtain permission from the license holder to reproduce the material. To view a copy of this license, visit <http://creativecommons.org/licenses/by-nc-nd/4.0/>

© The Author(s) 2018

Supplementary Information accompanies the paper on the Molecular Psychiatry website (<http://www.nature.com/mp>)